

Contents lists available at ScienceDirect

International Journal of Disaster Risk Reduction

journal homepage: www.elsevier.com/locate/ijdrr





Evaluating education disruption by integrated school and road infrastructure system analysis

Dina D'Ayala ^a, Rafael Fernández ^{a,*}, Ahsana Parammal Vatteri ^a, Zaishang Li ^a, América Bendito ^b, Soichiro Yasukawa ^b

- ^a UNESCO Chair in Disaster Risk Reduction and Resilience Engineering, Department of Civil Environment, and Geomatics Engineering, University College London, London, United Kingdom
- ^b UNESCO Unit for Disaster Risk Reduction, Paris, France

ARTICLE INFO

Keywords:
Education service interruption
Natural hazards
Systems resilience
Bayesian network
Agent-based modelling

ABSTRACT

Public education is considered a fundamental service governments should offer to their population. Nonetheless, in the occurrence of natural hazard events, it is often disrupted, as the school infrastructure gets damaged. Besides the physical damage to school buildings, factors such as the inability to commute also affect the capacity to restart classes. In destructive events, the commuting capacity can be affected by the structural damage of bridges, or by the inability to transit over blocked roads. In this context, the main objective of this research is to develop a methodology able to evaluate the risk of disruption to education caused by earthquakes and floods affecting both the physical school infrastructure in a region, and the road network that serves it. The proposed method integrates a Bayesian Network, a Monte Carlo simulation and an Agent-Based model to assess the interruption of the educational service. A substantial novelty of the proposed model is the integration of the community social vulnerability parameter with the physical vulnerability of the buildings, as both contributing to determine the operational capacity. This method is demonstrated via a case study of the province of San Pedro de Macoris in the Dominican Republic. Results show that the implementation of retrofitting strategies in school buildings and bridges can drastically reduce the education interruption time. Such improvement can be communicated with a simple, relatable cost metric-the cost of reducing one day of interruption per student-to provide meaningful insights for non-technical audiences and decision makers.

1. Introduction

Public education is one of the most important services that a government can offer to its population. However, in many countries worldwide it is often disrupted by the occurrence of natural hazardous events. The *Report of the United Nations High Commissioner for Human Rights* on the "Impact of climate change on the equal enjoyment of the right to education by every girl", states: "Extreme weather may damage or destroy school buildings, facilities and transport, thus disrupting children's access to education. Schools may also be closed when school buildings are used as emergency shelters" [1]. The impact of these interruptions can be devastating to children's education and future. Earthquakes can generate damage in structural and non-structural components, which take time to

E-mail address: rafael.fernandez@ucl.ac.uk (R. Fernández).

https://doi.org/10.1016/j.ijdrr.2025.105588

^{*} Corresponding author.

repair. The 2010 Haiti Earthquake damaged more than 4,000 schools, affecting around 2.5 million students for more than 3 months [2]. Likewise, the Puerto Rico 2020 earthquake, interrupted the educational service for more than two months [3]. Even relatively moderate earthquakes, such as the Dominican Republic, Puerto Plata earthquake in 2003 [4] can have severe impacts in educational infrastructure. Floods also cause great disruption to educational services. Munsaka & Mutasa [5] presented an analysis showing the impact of fluvial and flash floods in the African continent, identifying school accessibility as the major obstacle to education continuity. They emphasize how the poorest communities are the most affected, living in vulnerable houses and using vulnerable infrastructure in highly hazardous zones. Similarly, the Jakarta, Indonesia, 2013 floods resulted in an interruption of educational service up to 30 days, while repair to the structural damage of school facilities took between 26 days to six months, the availability of funds being the major hurdle [6].

Long disruptions present great risks to the students. Education interruption can result in child labour, early marriage, and exploitation among other undesired impacts [7]. Also, long interruptions increase the risk of larger quotas of education dropout, affecting future income and the development of nations [2]. For instance, Thamtanajit [8] collected empirical evidence of the impact of the 2011 floods in Thailand on student achievement, resulting in a negative impact on most test scores for grades 6 to 9 in affected schools. Gibbs et al. [9] showed that schools affected by wildfires in rural Victoria, Australia, presented a reduction in reading and numeracy scores compared to schools in unaffected areas, with affected children impacted suffering post-traumatic stress disorder (PTSD), generating difficulties in attention, speed of processing, problem-solving, etc. With reference to the Yogyakarta earthquake in 2006, the long-term effect of school disruption has been quantified in terms of lost years of schooling (in terms of both drop in enrolment and completion) resulting in substantial loss of human capital [10]. The way in which hazards of different nature and different magnitude affect the education systems should be further researched, also taking into account the specific socio-cultural and economic context. It is critical to understand how rapid recovery affects long terms impact, however this is beyond the scope of this study. In addition to the adverse effects of education interruption, school infrastructure resilience is also essential to prevent life loss and to ensure it can be used as shelter [11,12].

Therefore, reducing the interruption of educational services caused by natural hazards should be a major objective for national governments. This ability to recover in time is known as resilience. The United Nations Office for Disaster Risk Reduction offers a definition of system resilience against natural hazard as timely and efficient recovery of its essential basic structures and functions [13]. Few approaches have been proposed to quantify the level of resilience for school buildings [14]: defined a resilience index accounting for structural, non-structural, functional components, and services, and verified its applicability by studying a sample of 400 school facilities in Yazd, Iran [15,16] implemented a similar approach, for preliminary assessment of the educational sector seismic resilience in Calabria, Italy, considering, besides structural, non-structural and equipment components, also location and commute routes. The proposed set of parameters can be easily identified from a census information or an Education Management Information System (EMIS), as they refer mainly to education characteristics of the school. However, while the data required might be relatively easy to collect, the level of reliability of the results is generally low.

Alternatively, approaches can be based on numerical modelling [17]: evaluated the functionality, recovery and resilience of a school system following a severe earthquake in a simulated testbed, by developing a Markov chain stochastic model coupled with a dynamic optimisation model to determine the school recovery trajectory. Seismic resilience can also be computed as a by-product of probabilistic risk assessments, including the assessment of the physical fragility and vulnerability of structures, to identify the economic, human and time losses. Examples of this approach have been implemented in Mexico [18], Iran [19], Portugal [20]. A comprehensive review of this and other methods can be found in Ref. [21]. The main challenge of these approaches is the availability of complete and robust data.

Moreover, continued delivery of the education service relies as much on resilient schools, as on the functionality of other infrastructure systems. For instance, the ability to commute to schools after a hazardous event is critical to the continuity of the education offer. Therefore, the interruption of a road or a bridge damaged by a natural event, may disrupt several services by isolating a community and affecting the rapid response for effective recovery [22]. The relationship between the infrastructure network and education quality has been previously studied, as this affects the possibility of students to attend in-person education [23–25]. However the relationship between education interruption and the hazard specific resilience of school and road systems, including the interaction of recovery agents has not been sufficiently investigated, and neither the uncertainties associated with it appropriately quantified. Therefore, the main objective of the present study is to develop a methodology, applicable to earthquakes and floods, to evaluate the interruption of education services at a territorial scale, accounting explicitly for the effects of the transportation infrastructure functional interruption on such recovery. The methodology is presented in Section 2, while its applicability is discussed in Sections 4 and 5 through application to a case study in the province of San Pedro de Macoris in the Dominican Republic, introduced in Section 3. For the purpose of reproducibility more details on the data used can be found in the UNESCO report: D'Ayala et al. [26].

2. Methodology

2.1. Overall framework

The proposed methodology consists of a probabilistic resilience framework for system performance and recovery analysis. In a nutshell, the first step identifies the probability of operational capacity of school and transportation infrastructure considering also the possible use as shelters of school buildings. This is calculated using a Bayesian Network (BN) that correlates the hazard level through an intensity measure, to the response of the infrastructure expressed in terms of fragility functions (these compute the probability of the structure exceeding a given damage state, for a set value of the hazard intensity measure) [27]. In a second step, to consider the

intrinsic uncertainty in this process, the results of the BN are used to generate a set of stochastic simulated operational capacity realisations for infrastructure components using a Monte Carlo approach (MC) [28]. Finally, each simulated scenario serves as input to an Agent-based model (AB) which quantifies the recovery time of the system, given a set of recovery strategies and a set of behavioural constraints for the Agents (Fig. 1) [29].

Studies coupling these three modelling techniques are not common, although some combination of them has been employed previously. For instance Ref. [30], utilised a Bayesian cognitive map as the decision model in an agent-based model, to elicit probabilities of making a positive decision, allowing to incorporate real-world uncertainty in the context of water resource management. Recognising the flexibility of the probabilistic directed graphic BN, Abdulkareem et al. [31] used data driven BNs to support agent decisions in a spatial AB model. They trained the BN alternatively with sparse survey data and with data and expert knowledge, to refine the agent behaviour. The procedure was applied to model the spatial distribution of the cholera epidemic in Ghana. Similar combinations of BN and AB models have been used in studies to develop spatial models of land-use change affected by human behavioural choices [32] or flood risk assessment and management [33] and more generally in ecological sciences and environmental management [34]. In the context of disaster risk reduction, BN approaches have become increasingly popular in determining the resilience of infrastructure systems exposed to single or multiple natural hazards [35–37]. Similarly, the use of AB models to study infrastructures and social systems post-disaster recovery trajectories has seen a marked increase [22,38,39], encompassing different extent of system dependence, interconnectivity and type of hazard. Yet, coupled infrastructure systems recovery for multiple hazards, in the context of school infrastructure resilience, is, to the authors' knowledge, not been investigated.

Therefore, the present probabilistic framework estimates the disruption to education due to a given hazard to quantify the resilience of coupled school-road networks by modelling causal effects and correlation between physical, functional, and social vulnerability associated with each infrastructure component. It explores strategies for enhanced resilience by tracking the recovery trajectory according to decisions taken by two agents, namely the School Operator (SO) and Road Operator (RO). The flow chart in Fig. 1 show the flow of information through the different modelling components. The main output of this integrated approach is the time of interruption of the educational service. The analysis is conducted for the current physical state of the two infrastructure systems and hypothetical retrofitting scenarios. Comparing the results highlights the reduction in interruption of educational service that can be attained by implementing a specific retrofitting strategy, given a level of financial investment. This information represents a key metric for decision-makers in the development of school infrastructure management plans, as it links directly the days of school loss per student to the investment made in the infrastructure. In the remainder of this section details of the three main steps of the methodology are reviewed and discussed.

2.2. Bayesian network and social vulnerability

The BN framework proposed here comprises two acyclic graphs, for the school and the road infrastructure. The first (Fig. 2)

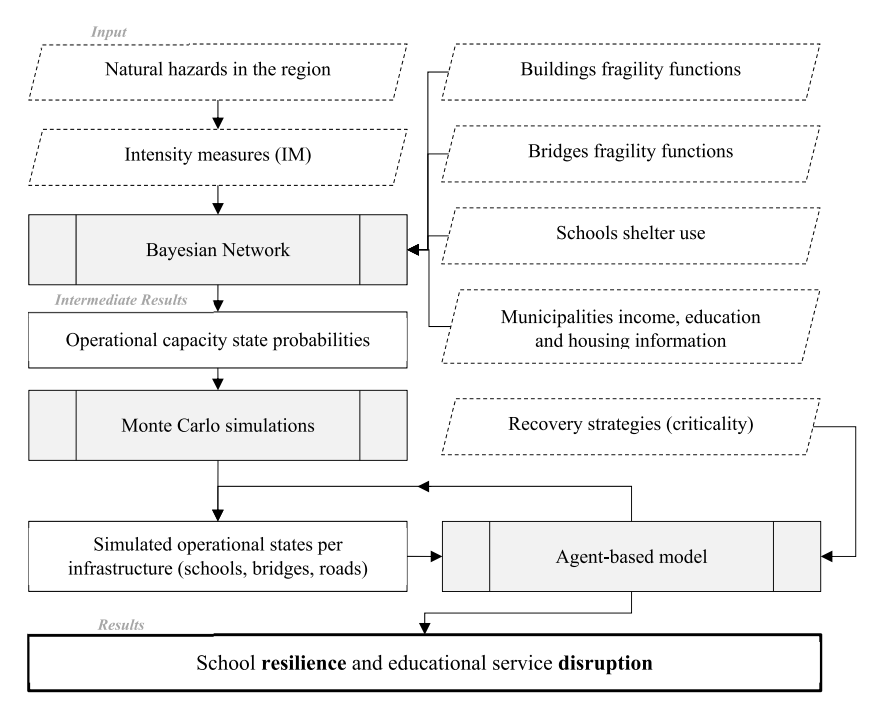


Fig. 1. Proposed methodology integrating Bayesian Networks, Monte Carlo simulations, and Agent-Based models, and data flow through the components.

estimates the states of the operational capacity of schools caused by the impact of the hazards and their possible use as shelter. The parent node is the probability of the hazard intensity at the school location, which, by use of fragility functions, provide the probability of specific damage states for each school building and then integrates them to functional states at the school level (see Fernández et al. [40]) and at municipality level as further explained in Section 4. Local authorities often identify certain schools as possible shelters in the aftermath of disasters, thus indicating an initial probability of a school being a shelter for the system analysis. The BN further correlates the probability of social vulnerability (SV) states for the community the school pertains to, affecting the likelihood of the school being used as a shelter. These factors, i.e. the functional state probability from the physical damage, the initial shelter state probability and the influence of social vulnerability status on the need for shelters, are used to calculate the school's or municipality's operational capacity state probability and associated duration of disruption (Fig. 2). Further details on this approach and an example of its application can be found in Parammal Vatteri et al. [37].

A substantial novelty of the proposed BN model is the integration of the community social vulnerability parameter with the physical vulnerability of the buildings, as both contributing to determine the operational capacity. Evidence suggests that disadvantaged communities disproportionately receive the negative impacts of natural hazards [41–43]. To calculate this effect, a number of factors that influence the vulnerability are identified in the literature, including economic status, education level, age profile, disabilities, minority status or the presence of vulnerable groups, housing type, access to transportation etc. [44–46]. An aggregation of these factors to generate a composite index is most used as a proxy of the social vulnerability of a community [47]. Several approaches to estimating such a synthetic social vulnerability index exist, such as principal component analysis [48], data envelop analysis [49], analytical hierarchy process [50] or multi-criteria analysis [51]. In regional analysis, such as the scale of the present study, social vulnerability levels can be computed using a multi-criteria procedure, such as the one developed by Lee [51].

Instead of attempting an exhaustive description of the complex interplay of factor determining social vulnerability, the approach in this study is to define the relative social vulnerability of the communities served by the school infrastructure, through limited, yet critical parameters identified from the literature review and typically available as open-source data. Adopting the approach to represent social vulnerability as an aggregation of selected factors without weights [47,50], the BN analysis in this study identifies *Income, Education* and *Housing* as parent nodes of social vulnerability (Fig. 2) in the context of disaster preparedness, recovery and resilience. Since the use of schools as shelters is an important criterion in deciding the operational capacity of schools in delivering education, these factors of social vulnerability that directly contribute to the need for shelter are relevant to the study. Economically poor sections of the community are more likely to suffer from a damaging event, owing to the reduced risk perception, preparedness and ability to respond and recover [41,52]. Formal education is frequently linked to social vulnerability [52] as better education can lead to reduced vulnerability owing to the potential to a stable income and greater ability to cope with the physical and psychological effects of disasters [53–57]. *Housing* is an indicator of affordability, quality and stability, whit direct affect to vulnerability (loss of abode), besides indicating lower disaster preparedness and ability to recover [58], and hence shelter need.

In this specific study, the variables *Income* and *Education* are defined to have three qualitative states, namely, *low*, *medium*, and *high*, based on the indicators available in the census analysed, although others can be used in a similar manner. The fraction of the population classified in general poverty is considered to have 'low' income while those with private cars are considered to have 'high' income. The remaining population is categorized in the medium income level. Similarly, the fraction of illiterate population and those with university degrees are considered to have 'low' and 'high' states of education, respectively, while the remaining population in between these two states are assumed in the 'medium' education state. The variable *Housing* is defined to be in either 'good' or 'bad' state depending on the quality of construction materials, for instance, timber houses with soil floors are considered 'poor' whereas,

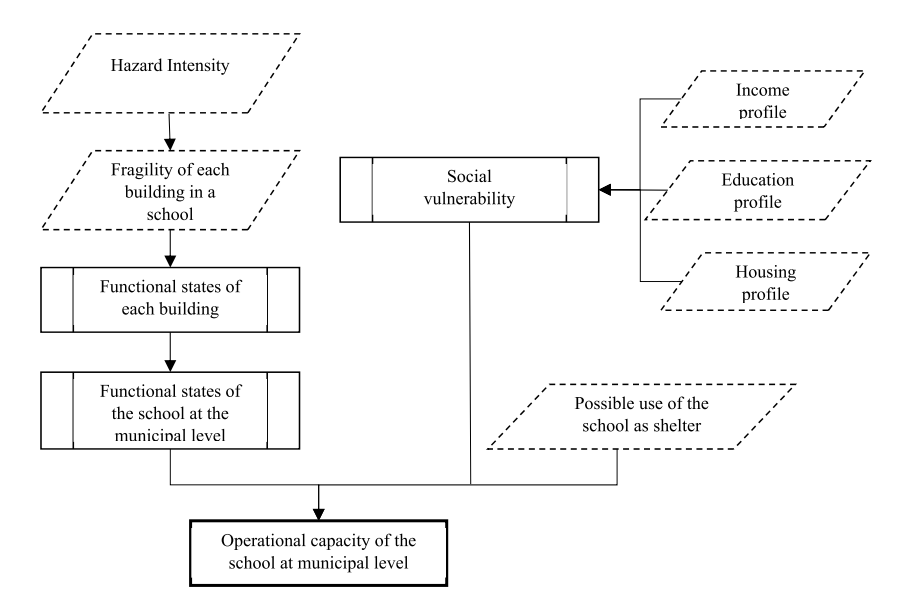


Fig. 2. Simplified Bayesian network for a school exposed to natural hazard.

standard construction materials such as bricks and concrete are considered 'good'. Their statistical distributions, based on publicly available census data aggregated at the municipality level are sampled to define the probability of each being in one of the qualitative states defined.

To include these parameters in a synthetic mode in the BN, while preserving the specific probabilistic distribution observed for each of them, a Conditional Probability Table (CPT) is developed (Table 1), which establishes possible outcomes of the level of SV given the specific states of the three parameters. One end of the spectrum where all the parent indicators are in the 'worst' or 'poorest' possible state is defined as having 'high' SV, as this combination indicates the lack of capacity to quickly recover from a disaster autonomously or through government assistance as lacking the tools to access the aid and fund options [59] Additionally, the poorest states of the parent factors result in a compounded state of overall high SV, for instance, low-income households tend to live in poor quality houses and be less educated [59]. The complex underlying implications of these factors which are not explicitly modelled here, are incorporated in the broad range of 'moderate' SV state, which is defined for all other combinations of the parent states, For instance, any of the three parent factors being in a medium or good state may indicate sufficient resources to more easily access aid, recovery and reconstruction loans, and insurance coverage [59]. Decent income, education or adequate housing are also shown to result in better disaster preparedness as compared to the poorest section of the community [58], in terms of means for immediate sustenance, information and financial resources. The other end of the spectrum is the 'low' state of SV, which is assumed when the parent variable states are all in the medium to high range, indicating the capacity to respond and recover from a disaster relatively unharmed. The associated probability of three possible states of SV in a given municipality is then calculated as a conditional probability on the parent state probabilities through BN inference. Even though there could be correlations between the factors, it is not considered in this analysis for the lack of sufficient information.

It is acknowledged that the conditional definitions, although guided by evidence in literature, are subjective to the analysts' decision, and they can be updated depending on availability of case-specific information. The advantage of the BN approach is that it sets a platform to incorporate such subjective knowledge and qualitative information into the analysis framework [60,61] to make inferences and retains the flexibility to test different hypotheses.

It is observed that people who seek shelter in public facilities such as schools are more likely to have low socio-economic status [59]. As a result, a connection between higher probability of education interruption for students from socially vulnerable neighbourhoods has been also observed in post-event recovery, as schools are required to function as shelters [42,62]. As shown in Fig. 2, the SV indicator affects directly the probability of the school functional status as shelter, also conditioned by the physical state of the school, leading to five possible operational capacity states of each school: non-damaged and used as short-term shelter, non-damaged and used as long-term shelter, intact (non-damaged and not used as shelter), partial operational capacity (associated with moderate damage) and shutdown (associated to extensive damage).

The road BN object estimates the probability of three states of connectivity of the schools on account of damaged road network, given a probability of hazard intensity (Fig. 3). Due to the different nature of disruption caused by seismic and flood hazards, the study assumes that each hazard affects only one type of component of the road network, leading to two independent branches of the BN. For seismic hazard, structural damage to bridges is considered as cause of disruption. Therefore, the inputs to the road BN are the fragility functions for bridge typologies and the output is probability of operational capacity of the road paths (Fig. 3). Conversely, inundation of road segments is the concern under flood hazard, given the low level of inundation expected. The susceptibility to flood damage of the road segments determines the operational capacity of the paths connecting the schools. The effect of earthquakes on roads located on top of seismic faults, and of flash floods on bridges are out of the scope of this paper. Nonetheless, the BN allows to add links between each hazard and each component to analyse consecutive events and their combined effects on both school and road infrastructure [35,63].

2.3. Monte Carlo simulations

The output of the two BN objects is the probabilities of each operational state of the school and road infrastructure components, considered independently. However, to assess the educational interruption time, it is necessary to identify a specific operational state of the whole schools and road system. This is conditioned by the aleatory nature of the hazard intensity, the exposure and the vulnerability of the physical systems, as well as of the social vulnerability. To propagate such uncertainty to establish the resilience of the educational services, the stochastic nature of the problem is preserved by considering a sufficiently large number of simulations using the Monte Carlo (MC) approach. This allows to determine specific instances (simulations) based on the probability distribution of one or more random variables [28]. It is worth noting that more simulations will result on a better representation of the distribution. MC simulations are particularly appropriate in the context of modelling of risk assessment, due to the dynamic complexity, incomplete information, and limited accuracy of prediction models [64,65]. MC is commonly used to model earthquake hazard and risk [66], as well as landslides, affected both by hydrometeorological and geophysical hazards [67–69]. MC simulations are recommended to

Table 1Conditional probability table for social vulnerability.

Income, Education and Housing	Social Vulnerability
Income and Education are medium or high, and Housing is good	Low
Income or Education are medium/high, or Housing is good	Moderate
Income and Education are low, and Housing is bad	High

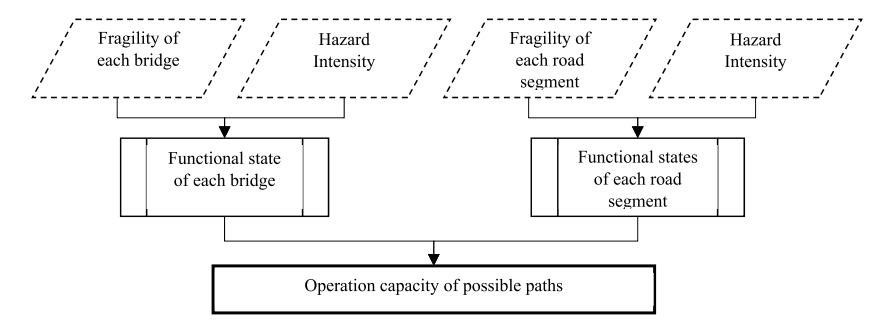


Fig. 3. Simplified Bayesian network for a road network exposed to natural hazard.

propagate the uncertainty associated to exposure and vulnerability, as shown in D'Ayala et al. [70], and to simulate current and future possible exposure models for risk assessment purposes [71,72].

In this study, the instances will be sampled, based on the probability distribution of the operational conditions obtained in the BN for each element. The type of elements considered in the model varies according to the resolution of the analysis. For instance, the model can identify school buildings and bridges as components or can aggregate the components by school facility or municipality depending on the scale of the model. Each simulation is evaluated by the Agent-based model presented in the following section. The MC simulations in this framework works as the link between the Bayesian Network and the Agent-Based model.

2.4. Agent-based model

The Agent Based model's objective is to track the functionality recovery of the integrated school-road networks, affected by each hazard. It models the interactive decision-making of relevant actors in the recovery process. In this application a School Operator (SO) and a Road Operator (RO), are chosen as the agents, whose actions are shaped by a set of pre-defined, adjustable behavioural attributes [22]. Fig. 4 provides the logic of the AB model. Both SO and RO start in an idle state. After the hazard occurrence, they will inspect the probability distribution generated in each MC simulation to assess the operational state of the system. The progress of each operator will be conditioned by a set of priorities/criticalities of the infrastructure, which define the recovery sequences of the infrastructure that the operators will follow. The criticalities can be set and ranked by different criteria of interest like the student numbers of the schools or the damage states of the infrastructure. They can be set at the beginning of the recovery phase or updated at each iteration.

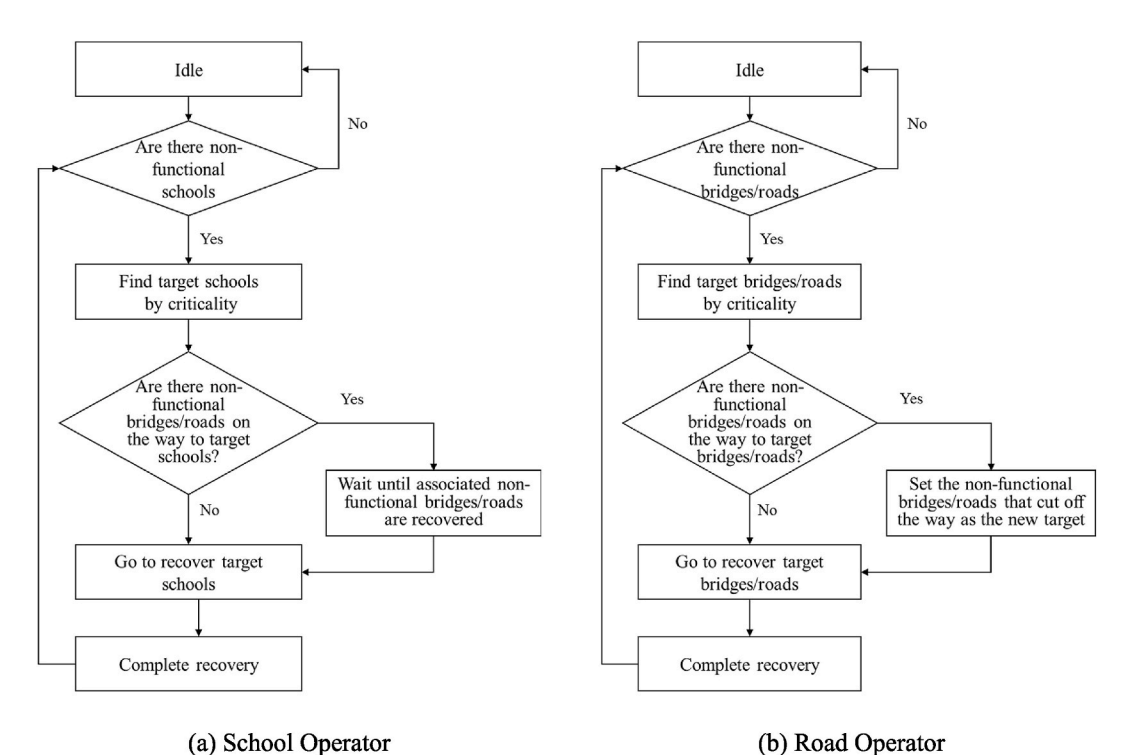


Fig. 4. Agent Based Model Operators logic.

More details can be found in sections 4 and 5. The interaction between the two operators is determined by any instance of functionality loss by any bridge or road segments that hamper the SO recovery process, represented as a period of idleness of the SO, waiting until the associated bridges/roads are recovered by the RO. On the other hand, the RO will also be obstructed in its recovery plan by any non-functional bridge/roads on its path to any bridges/roads set as target. Therefore, the priority ranking for the RO, although set at the beginning of the recovery phase on the basis of holistic criteria, might need to be updated on the basis of local elements' functional states when the targets are re-set at each iteration, as shown in Fig. 4.

The AB model enables computing the return to the educational service over time. For each school recovered, the number of students with access to education will increase according to that schools' receptive capacity. The time to recovery is a function of the operational state of the school, the time that the SO takes to travel from one target to the next, impaired by the recovery of the road network. Moreover, the shelter use will also impair such recovery: the education function associated with the schools used as shelters will be recovered once the shelter use period has elapsed (either short-term or long-term). These schools however are intact and will not be attended to by the SO.

3. Case study: San Pedro de Macoris, the Dominican Republic

3.1. Province selection: San Pedro de Macoris

The public-school building portfolio of the Dominican Republic accounts for 18,280 units distributed around 6,000 school compounds attended approximately by 1.5 million students, according to the Government's National Office of Statistics (ONE) records for the year 2021. To demonstrate the method, the southeast province of San Pedro de Macoris was selected as a case study, considering the schools' available data and the relevance of earthquake and flood hazards for this province. The main city in the province has a population of 195,000 inhabitants and is situated 75 km east of the capital Santo Domingo. Two main rives flow in the province territory of approximately 150 square kilometres: rivers Higuamo and Soco. The province includes 288 school facilities, more than 1,750 km of roads, and 46 bridges.

3.2. Socio-economic characteristics

As mentioned in section 2.2, three socio-economic indicators are analysed: income, education and housing. The statistics for each of them are provided by the latest census [73] and presented in Table 2, subdivided into relevant attributes. The city of San Pedro de Macoris presents a better socio-economic profile than the other municipalities, showing a lower proportion of households in poverty, a lower illiteracy rate and a greater percentage of households with cars and good housing standards. On the other hand, Los Llanos and Ramón Santana show high percentages of households in general poverty, and the two higher illiteracy rates.

3.3. School infrastructure

The geographical distribution of the school facilities by municipality is shown in Fig. 5. A total of 288 schools with around 800 buildings accommodating about 80,000 students, are distributed in clusters within the main city and along the major roads extending into the inner part of the province Because the hazard is assumed as constant across the region, this clustering does not affect the results. The recovery time is proportional to the number of schools in each municipality. The distribution of school building typologies across the country is substantially classifiable in about 10 recurring blueprint typologies corresponding to successive construction programs of the Department of Education [74]. Each typology is assigned a taxonomic string, using the Global Library of School Infrastructure (GLOSI) seismic taxonomy classification system [75], which summarises their essential structural characteristics determining their seismic performance. A representative picture of each typology, its GLOSI taxonomy, its proportional occurrence at the country level, and associated seismic fragility function are presented in Table 3. Table 4 summarises the typologies distribution by municipality. The most recurring is the reinforced concrete RC3/LR/LD, the second most common typology across the country. The second typology at province level, RC3/MR/LD, common in Guayacanes and San Pedro de Macoris city, is the first across the country. The reinforced masonry typology RM/LR/LD is relevant in the rural municipalities of Guayacanes, Los Llanos and Consuelo. In San

Table 2 Municipality socio-economic classification.

Municipality	Income			Education			Housing	
	Low (general poverty)	Medium (remaining population)	High (with private cars)	Low (illiterate)	Medium (remaining population)	High (university or higher)	Poor (timber houses, soil floor)	Good (remaining houses)
San Pedro de Macoris City	41.50 %	46.40 %	12.10 %	8.40 %	82.34 %	13.38 %	2.00 %	98.00 %
Guayacanes	56.40 %	33.60 %	10.00 %	12.90 %	86.00 %	5.05 %	2.30 %	97.70 %
Los Llanos	70.00 %	24.20 %	5.80 %	20.90 %	81.76 %	4.73 %	18.10 %	81.90 %
Quisqueya	60.40 %	34.10 %	5.50 %	13.10 %	85.52 %	6.78 %	6.00 %	94.00 %
Consuelo	48.50 %	45.60 %	5.90 %	12.60 %	83.65 %	8.79 %	4.90 %	95.10 %
Ramón Santana	74.60 %	21.10 %	4.30 %	22.60 %	80.96 %	3.53 %	11.90 %	88.10 %

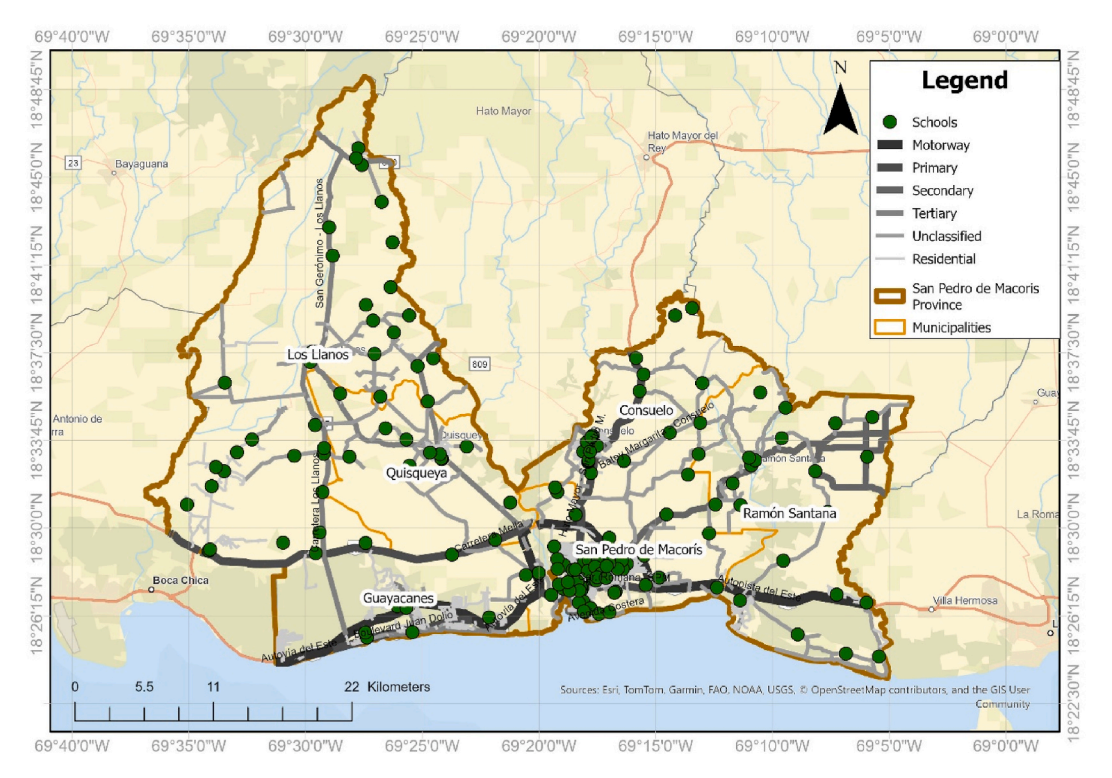


Fig. 5. School facilities and roads in San Pedro de Macoris.

Pedro de Macorís city, bare frames reinforced concrete typologies RC1/MR/HD and RC1/LR/HD (PNEE) have considerably higher occurrences than in other municipalities. This typology has been implemented from 2011 onwards, and its structure complies with the latest national building code, updated after Haiti's 2010 earthquake. Therefore, these buildings are less vulnerable than other typologies. RM/LR/LD Johnson typology, a vulnerable older reinforced masonry typology, is common mainly in Ramón Santana. Finally, timber frame (TF/LR/LD) and poor design reinforced masonry, PIDE (RM/LR/PD), although a minority across the province, are the country's most vulnerable typologies.

Since most of these typologies present a high vulnerability against earthquakes, their structural retrofitting is considered an essential strategy to improve the school infrastructure resilience as further discussed in Section 4.3. A specific study on the most appropriate type of retrofitting and associated cost for each typology conducted by the authors, is reported in Fernández et al., [74].

3.4. Bridge and transportation infrastructure

In addition to the school infrastructure data, the road network is analysed to identify the connections between schools. This analysis is fundamental to developing the proposed model to assess the disruption of education following natural hazards, since the transport infrastructure presents a high level of risk, as evidenced by the Interamerican Development Bank [76]. The road exposure model consists of the primary and secondary roads and the bridges that connect them. For the roads, several characteristics shall be identified such as the number of lanes, the paving material and its condition, among others. The road classification was obtained from OCHA Humanitarian Data Exchange [77] (Fig. 5). For the bridges, characteristics such as the number of spans, the bridge substructure and superstructure typologies and materials, among others, are used to evaluate their vulnerability. From data available, it can be concluded that one third of the road network is sited in San Pedro de Macoris City. Conversely, in rural areas, the scarcity of roads and bridges generates critical situations, resulting in the possible isolation of schools and populations, if one segment fails due to a damaging hazard event.

Eleven bridges critical to the school infrastructure, are identified in the province. These bridges were visited by The National Office for the Seismic Evaluation and Vulnerability of Infrastructure and Buildings (ONESVIE), photographs were gathered with the use of a drone, to identify their typology and condition. This is complemented with aerial information available online (e.g. Google Maps and Google Earth Pro). The seismic fragility model established by Nielson and DesRoches [78] is employed to determine damage probabilities, using fragility functions calibrated on results of the project SIGP (Colombia National System for Managing Bridges) for Colombia [79] (see Table 5). For "cable-stayed" bridges the fragility functions developed by Wu et al. [80] are used.

Interventions on bridges are considered in the model to assess the impacts in the reduction of the disruption of education after the occurrence of hazard events. For this process, the reduction in vulnerability and the costs of investment are based on the study developed by Universidad de Los Andes et al. [79]. The intervention costs were then calibrated using data on investment on bridges in

Table 3 Index buildings in the Dominican Republic. Adapted from Fernandez et al. [74].

Local typology name	Primary parameters GLOSI taxonomy string ^a	Percentage at country level	Representative picture	Seismic fragility function Green: Slight damage, Blue: Moderate damage, Orange: Extensive damage, Red: Collapse
1erBID	RC3/LR/LD	18.31 %		1.0 0.8 0.6 0.6 0.0 0.0 0.0 0.0 0.0 0.0
SEE	RC3/MR/LD	39.40 %		1.0 0.8 0.6 0.0 0.0 0.0 0.0 0.0 0.0 0.0
PNEE LR	RC1/LR/HD	2.58 %		1.0 0.8 0.6 0.0 0.0 0.0 0.0 0.0 0.0 0.0
PNEE MR	RC1/MR/HD	12.16 %		1.0 0.8 0.0 0.0 0.0 0.0 0.0 0.0 0
Jhonson	RM/LR/LD	5.81 %		1.0 0.8 0.0 0.0 0.0 0.0 0.0 0.0 0
PIDE PD	RM/LR/PD	0.93 %		1.0 0.8 1.0 1.0 1.0 1.0 1.0 1.0 1.0 1.0
PIDE LD	RM/LR/LD	14.30 %		1.0 0.8 0.0 0.0 0.0 0.0 0.0 0.0 0

(continued on next page)

Table 3 (continued)

Local typology name	Primary parameters GLOSI taxonomy string ^a	Percentage at country level	Representative picture	Seismic fragility function Green: Slight damage, Blue: Moderate damage, Orange: Extensive damage, Red: Collapse
Timber	TF/LR/PD	1.56 %		0.8 0.6 0.6 0.0 0.5 1.0 1.5 2.0 2.5 PGA [g]

^a Acronyms in the Taxonomy: RC3: RC framed construction with short columns, RM: Reinforced masonry with concrete blocks in cement mortar, RC1: Bare framed construction, TF: Timber Frames, LR: Low-rise, MR: Mid-rise, HR: High-rise, PD: Poor design, LD: Low design. MD: Medium design, and HD: High design. For more information on this classification see Ref. [63].

Table 4
School building typologies distribution in the seven municipalities in San Pedro de Macoris.

Typology	Quisqueya	Guayacanes	San Pedro de Macorís (City)	Los Llanos	Ramón Santana	Consuelo
1erBID/RC3/LR/LD	42 %	32 %	27 %	47 %	31 %	24 %
SEE/RC3/MR/LD	12 %	29 %	24 %	10 %	8 %	15 %
PNEE/RC1/LR/HD	19 %	9 %	18 %	6 %	10 %	12 %
PNEE/RC1/MR/HD	7 %	6 %	11 %	7 %	8 %	24 %
Johnson/RM/LR/LD	12 %	0 %	6 %	7 %	23 %	4 %
PIDE/RM/LR/PD	0 %	0 %	0 %	1 %	4 %	0 %
PIDE/RM/LR/LD	5 %	24 %	13 %	17 %	8 %	21 %
Timber/TF/LR/PD	5 %	0 %	1 %	4 %	6 %	0 %

San Pedro de Macoris province [81] provided by the Ministry of the Presidency of the Dominican Republic.

3.5. Seismic hazard

The island of Hispaniola (on which the Dominican Republic and the Republic of Haiti are situated) is located on the border between the Caribbean and North American plates, a region that generates a complex tectonic system with a large number of faults, creating a seismically active strip along the plate boundary. The global earthquake catalogue [82] records many high-magnitude events in the region. The 2010 Mw = 7.0, Haiti earthquake, (January 12, 2010), although highly destructive in Port-au-Prince was moderately felt in the Dominican Republic. Similarly, the 2021 M7.2 Haiti earthquake, had minimal consequences in Dominican Republic. The most damaging recent earthquake in the Dominican Republic occurred in 2003 in Puerto Plata. According to EM-DAT, it caused 3 fatalities and more than 2,000 people were affected [83]. School infrastructure was heavily affected, as recorded by Lopez & Martínez [4], particularly for the two-story reinforced concrete buildings locally known as SEE (see Table 3). Several structural deficiencies were identified such as short column, weak column–strong beam, and weak floor.

Considering the high seismicity of the region, several international studies have been conducted to understand the seismicity of the Dominican Republic [84–89]. The most recent is the one developed by GEM & USAID [84], which includes an updated earthquake catalogue and ground motion prediction equations.

Since the present study focuses on the San Pedro de Macoris province, it is important to understand the level of hazard, including acceleration and displacement in this region. However, given the level of resolution of available seismic hazard models and the lack of micro-zonation studies, the acceleration assigned to the region of analysis is assumed to be uniform. Since the development of a hazard model is out of the scope of this project, it taken as an input from the GEM & USAID analysis [84]. Table 6 presents the corresponding PGA and the Spectral acceleration (Sa) for two stochastic scenarios, one moderate and one extreme. The moderate scenario is based on the probabilistic hazard map with 10 % probability of exceedance in 50 years (equivalent to 475 years of return period – see Ref. [84]), while the extreme scenario is based on 2 % probability of exceedance in 50 years (equivalent to 2,500 years return period).

3.6. Flood hazard

Floods are a major natural hazard in Dominican Republic. They cause most of the natural hazard-related deaths, and the majority of damages to residential buildings, both at the national level and in the province of San Pedro de Macoris [90]. Tropical storms such as Franklin (2023), Grace (2021), and Laura (2020) have affected the country generating damage to infrastructure and human losses. A number of studies address flood susceptibility in the Dominican Republic [91–94]. The one by Rivera & Hernández [91], developed with the support of the Ministry of Environment and Natural Resources, while is the most updated, does not establish a probabilistic relationship between flood depths and return periods. Therefore, the model provides only a susceptibility map, as shown in Fig. 6. According to Ref. [95] a water depth of 0.25m shall be expected for a flood generated by hurricane-rainfall with a return period of 50

Table 5
Bridges in the Dominican Republic. Typologies and fragility functions adapted from Nielson & DesRoches [78] and Universidad de Los Andes, Universidad Javeriana & INVIAS [79].

Typology	Occurrences at province level	Representative picture	Seismic fragility function (from Nielson & DesRoches [78] unless specified otherwise). Green: Slight damage, Blue: Moderate damage, Orange: Extensive damage, Red: Collapse
Multispan simply supported concrete girder (MSSS1 concrete)	1		1.0 0.5 0.0 0.0 0.0 0.5 1.0 1.5 2.0 2.5 PGA [g]
Multispan simply supported slab with supporting frames (MSSS2 Concrete)	4		1.0 0.8 0.0 0.0 0.0 0.5 1.0 1.5 1.5 1.5 1.5 1.5 1.6 1.5 1.6 1.5 1.6 1.6 1.6 1.6 1.6 1.6 1.6 1.6 1.6 1.6
Multispan simply supported slab (MSSS slab)	1		0.8 0.8 0.0 0.0 0.0 0.0 0.0 0.0
Multispan continuous concrete girder (MSC concrete)	1		1.0 0.8 0.0 0.0 0.0 0.0 0.5 1.0 1.5 2.0 2.5 PGA [g]
Multispan continuous steel girder (MSC steel)	1		1.0 0.8 1.0 1.0 1.0 1.0 1.0 1.0 1.0 1.0
Single span concrete girder (SS concrete)	2		1.0 0.5 1.0 0.5 0.0 0.0 0.0 0.0 1.0 1.5 1.5 1.5 1.5 1.5 1.5 1.5 1.5

(continued on next page)

Table 5 (continued)

Typology	Occurrences at province level	Representative picture	Seismic fragility function (from Nielson & DesRoches [78] unless specified otherwise). Green: Slight damage, Blue: Moderate damage, Orange Extensive damage, Red: Collapse
Cable-stayed bridge (CS)	1		1.0 0.8 1.0 1.0 1.0 1.0 1.0 1.0 1.0 1.0

Table 6Seismic scenarios considered in the analysis.

Scenario	Scenario Equivalent Return Period [years]		Sa(T=0.2s) [g]	Sa(T = 1.0s) [g]
Moderate	475	0.25	0.6	0.2
Extreme	2475	0.6	1.2	0.4

years in the region. Therefore, the scenario used in this study assumes a water depth of 0.25m [95] in the susceptible areas for flooding [91]. This simplified approach is used as there are no models available with more precise information.

4. Interruption of education in seismic scenarios and resilience improvement

A simplified representation of the municipal nodes and connecting road network is mapped in Fig. 7. Municipalities are modelled by one node (e.g., Quisqueya, Guayacanes, and Consuelo) or two nodes (e.g., Los Llanos and Ramón Santana) according to their



Fig. 6. Flooding susceptibility map for San Pedro de Macoris.

territorial extension and distribution of population and school infrastructure. Due to its high population density and number of schools, the municipality of San Pedro de Macorís is subdivided into five interconnected nodes. Therefore, there are 12 municipality nodes (M1 to M12, Fig. 7). The distances shown on the links between nodes are the equivalent shortest distance of the existing roads connecting two nodes, including bridge crossing.

A sample of 160 public school facilities, comprising 525 buildings, for a total built area of 114,305 square meters is analysed. Each building is assigned a typology, a fragility function, a retrofitting technique with an estimated cost based on a previous study undertaken by the authors [74]. In order to facilitate the analysis at the province level, the fragilities of individual school buildings in each municipality are clustered at the nodes, and a cumulative fragility is assigned at each node by weighting the distribution of school building typologies in the municipality.

The BN analysis first computes for each node, the cumulative probabilities of the schools being in a given functionality state, given the probability of each building being in one of the four damage states identified by the cumulative fragility functions for each node, according to the following logical condition: damage states 'extensive' and 'collapse' to result in 'shutdown', damage state 'no or slight' to be considered as functionally intact and damage state 'moderate' to be taken as partially functional. Furthermore, in each municipality the government identifies a number of schools as possible shelters, providing a means to compute the initial probability of shelter use for each node. On the basis of the socio-economic states defined in Section 3.2, a probability for each social vulnerability state is calculated to each municipality and equally applied to all schools, as a conditional probability on the three parent state probabilities defined by the definitions in Table 1 through BN inference. These two probability conditions, combined with the probability of functionality states, determine the probability of a school being assigned a function of short-term or long-term shelter, or no shelter, as defined by the conditional definitions in Table 7. The functionality states and the shelter states determine the full gamut of operational states, as defined in section 2.2, then sampled in the MC simulations. Moreover, for each bridge in the network, with an assigned set of fragility functions, the BN analysis determines the associated probability of being in an operational state, given the damage states' probability.

The MC procedure then samples 1,000 possible realisation in accordance with the BN outcomes and feeds them to the AB model (see Fig. 1). The AB model assumes in all cases that SO and RO travel from a central coordination hub located in San Pedro de Macoris City and progress with the recovery action of the assets, as this is the largest city in the province, its administrative hub, and strategically located in its centre. The recovery sequences of each operator are determined initially by set criticalities. For the SO, the municipalities are ranked from high to low criticality by numbers of students; for the RO, the bridges are ranked from high to low criticality by the betweenness centrality of the link location of the bridge. The interactions between the two agents lie in the accessibility of the municipalities; the SO is not able to travel to a targeted municipality if the path is blocked by damaged bridges, needing recovery actions from the RO as shown in Fig. 7, depicting the topological road network and position of the bridges.

The time for recovery of education depends on many factors in the aftermath of a disaster, such as the immediate capacity of the government to react and the support given by the international community among other factors. This period can vary from a week, as

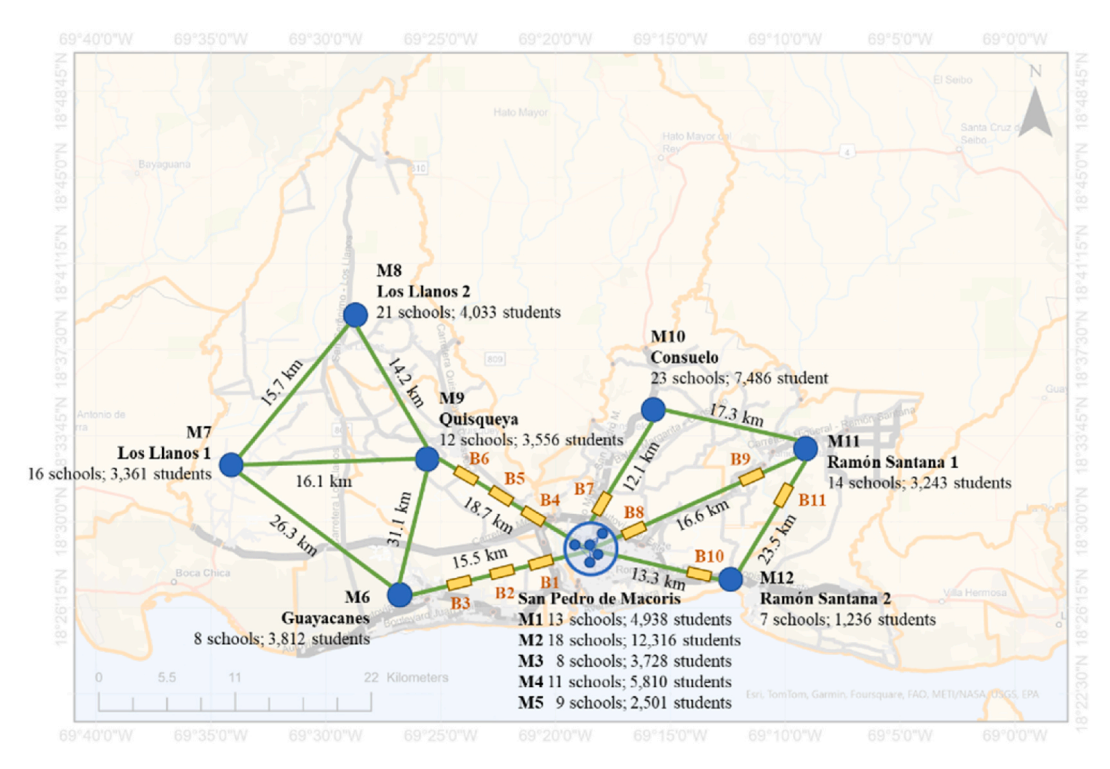


Fig. 7. Graph representation of the province network.

Table 7Conditional probability of short and long term shelter use.

Functionality State (FS), Shelter use (SH), Social Vulnerability (SV)	Operational capacity based on shelter use
No Shelter use OR functionality is affected Shelter use YES AND intact functionality AND high social vulnerability	Unaffected by shelter node, hence decided by functionality state (FS) Long shelter
Shelter use YES AND intact functionality AND social vulnerability is medium	Short shelter
Other combinations	Unaffected by shelter node, hence decided by functionality state (FS)

experienced in Japan after the 2011 earthquake, to more than 3 months, as shown in Haiti after the 2010 earthquake or the floods in the USA after hurricane Katrina in 2005 [2,96]. For example, in Türkiye the recovery of educational service in the affected areas with reinstatement of face-to-face teaching took approximately 7 weeks [97]. Lai et al. [98] provide anecdotal evidence of the high variability of school functional recovery after flooding with the shutdown period extending from 13 days to 1 year, even for schools affected by the same event. International organizations such as Save the Children aim to reinstall educational service after a disaster in less than one month [99]. Considering these examples and the fact that a robust data reference on school functional recovery is not available in literature, for this study the recovery of the education service is assumed to be two days for intact damage state (to allow the structures to be classified as safe and fully operational), two weeks for a partial operational state, and one month for a shutdown operation state. It is important to notice that the recovery of education in these cases is not associated with the repair and rebuilding of the school infrastructure, but to the re-instalment of educational services by implementing temporary measures such as tents or moving students to less affected areas, or minor cleaning and functional repairs. Considering this, the same recovery time is assumed for earthquakes and floods. This assumption is used as an input in this specific case study, but does not intend to be universal, as recovery times are socio-cultural and economic context specific. The two time periods assigned as possible use as shelters are obtained from the literature [17,67,100]. The recovery periods are summarized in Table 8. It is assumed that in each municipality the recovery activity will take places for all schools at the same time. This optimal condition might not reflect a real situation.

Similarly to schools, the same reasoning was implemented to identify the recovery time for bridges. In this case, besides the level of damage, additional factors such as the span length, the type of bridge, the soil characteristics, the location accessibility, and the available resources and coordination among others affect the time of recovery of the specific bridge. Usually, one or two days are taken for inspection, even when failures are not evident. For example, the Federal Highway Administration in the United States usually inspects bridges after earthquakes to ensure their safety, taking around 1 day as demonstrated during the 4.1 magnitude earthquake in East Tennessee [101]. When the level of damage is slight and not structural, repairs can take between one to four weeks as demonstrated during the Anchorage Earthquake in Alsaka where roads were repaired in 4 days [102] or after the July 2023 heavy rains in New York, where the Popolopen bridge was repaired after four weeks [103]. For major structural damage, or collapse, the repairs or reconstruction can take months or even years. However, in these situations, depending on the size and complexity of the bridging gap, temporary measures can be taken relatively quickly to ensure the recovery of service. In particular, the installation of temporary military bridges (e.g. a modular Bailey bridge) can be delivered in less than a month, including planning, procurement, transport, and installation. For instance, in New Zealand in 2023 after the collapse of a bridge due to floods, the installation of a short span temporary bridge took about one week [104], while a similar installation of a long-span temporary bridge in 2021 in the United Kingdom took about 2 months [105]. Considering these time frames, the assumptions for the bridge recovery are presented in Table 9.

4.1. Results of assessment

The results of the BN analysis regarding the probabilities of operational states in terms of damage and shelter use of the schools in each municipality are given in Tables 10 and 11 respectively, for the two seismic hazard scenarios. Likewise, the probabilities of the operational state of bridges are given in Table 12. A significant increase in the probabilities of partial operation and shutdown of both schools and bridges can be observed as the hazard intensity increases from moderate to extreme. Accordingly, the chances of the schools being used as shelters reduce.

Fig. 8 (a) and (b) show the trajectories of recovery of the school infrastructure operation under the two seismic scenarios considered. The vertical axis represents the percentage of students with access to education with time, being 100 % once recovery is complete, while the horizontal axis represents the recovery time after the event. Each chart indicates the recovery median trajectory and its range of results for all the MC simulations considered, highlighted by the colour-filled areas. This dispersion increases with the magnitude of the event and the progress of the recovery process. This reflects the uncertainties associated with the BN tree and provides a synthetic interpretation for decision-makers of the possible outcomes under realistic constraints.

Recovery times for schools.

Operational State	Time of education service interruption (days)
Intact	2
Partial	14
Shutdown	30
Short-term shelter	7
Long-term shelter	14

Table 9Recovery times for bridges.

Operational State	Time of interruption (days)
Intact	2
Partial	14
Shutdown	30

Table 10Probabilities of school operational state given functionality state.

· -	Moderate scena	Moderate scenario			Extreme scenario		
	Intact	Partial	Shutdown	Intact	Partial	Shutdown	
M1	0.669	0.294	0.037	0.161	0.391	0.449	
M2	0.824	0.162	0.014	0.142	0.369	0.489	
M3	0.875	0.121	0.004	0.235	0.501	0.265	
M4	0.950	0.045	0.005	0.232	0.388	0.380	
M5	0.776	0.175	0.050	0.281	0.394	0.325	
M6	0.782	0.211	0.007	0.112	0.420	0.468	
M7	0.810	0.164	0.026	0.123	0.599	0.278	
M8	0.679	0.273	0.048	0.079	0.529	0.392	
M9	0.829	0.128	0.043	0.214	0.487	0.299	
M10	0.772	0.212	0.015	0.135	0.490	0.375	
M11	0.597	0.307	0.096	0.085	0.452	0.464	
M12	0.806	0.145	0.048	0.241	0.388	0.372	

Table 11Probabilities of school functionality as a shelter.

ID	Moderate scenario			Extreme scenario		
	Not used as shelters	As short-term shelters	As long-term shelters	Not used as shelters	As short-term shelters	As long-term shelters
M1	0.733	0.000	0.267	0.936	0.000	0.064
M2	0.762	0.000	0.238	0.959	0.000	0.041
М3	0.690	0.000	0.310	0.917	0.000	0.083
M4	0.633	0.000	0.367	0.910	0.000	0.090
M5	0.715	0.000	0.285	0.897	0.000	0.103
M6	0.755	0.001	0.245	0.965	0.000	0.035
M7	0.486	0.004	0.510	0.922	0.001	0.078
M8	0.632	0.005	0.363	0.957	0.001	0.042
M9	0.767	0.002	0.231	0.940	0.001	0.060
M10	0.695	0.001	0.304	0.947	0.000	0.053
M11	0.821	0.007	0.172	0.975	0.001	0.024
M12	0.532	0.004	0.464	0.860	0.001	0.138

Table 12Probabilities of bridge operational states in terms of damage.

ID	Moderate scenario			Extreme scenario		
	Intact	Partial	Shutdown	Intact	Partial	Shutdown
B1	0.898	0.070	0.032	0.469	0.223	0.309
B2	0.852	0.089	0.058	0.419	0.206	0.375
В3	0.898	0.070	0.032	0.469	0.223	0.309
B4	0.111	0.244	0.645	0.004	0.030	0.966
B5	0.898	0.070	0.032	0.469	0.223	0.309
B6	0.836	0.126	0.039	0.424	0.301	0.275
B7	0.987	0.009	0.005	0.893	0.056	0.051
B8	0.987	0.009	0.005	0.893	0.056	0.051
В9	0.898	0.070	0.032	0.469	0.223	0.309
B10	0.652	0.138	0.209	0.115	0.102	0.783
B11	0.898	0.070	0.032	0.469	0.223	0.309

The median curves in Fig. 8 show for both scenarios that the first "recovery step" leads to 22 % of students regaining access to education, as M2 is the most critical municipality, ranking first by number of students. The longer delay before this first step under the extreme scenario corresponds to the higher probability of schools in partial or complete shutdown (see Table 10). The SO then heads

for the next ranked municipality, M10, but in doing so is substantially delayed by the recovery of bridge B7 on its path, which is a clear bottle neck, under both scenarios. The model is therefore able to clearly identify criticalities in both infrastructure systems that need attention.

4.2. Value of alternative recovery strategies

The recovery sequence shown in section 4.1 assumes that SO and RO carry out their activity following the criticality ranking criteria set for each of them. This is a naïve or baseline setting, denoted as MC1 for the municipalities and as BC1 for bridges. It is worth considering alternative ranking criteria to investigate how sensitive rapidity and recovery are to this early decision-making.

An alternative ranking of criticality for municipalities can be based on their damage states (denoted as MC2) – the municipality with the severest operational state is ranked the highest. As the operational state is a probabilistic variable set through the BN, the ranking may vary for MC realisations. For municipalities with the same state probabilities, the relative criticality will be set randomly. Regarding the criticality of bridges, an alternative option for ranking can be setting the recovery sequence of bridges "to follow" the recovery sequence of municipalities (BC2). In other words, the ranking of bridges will depend on the trajectory of the SO once the municipalities have been ranked. This imposes to get the bridges ready in advance for school recovery needs.

The above rankings can be set before the recovery phase and remain static throughout. Instead, a dynamic criticality approach for SO and RO can be set, which draws lessons from the "greedy algorithm" [106]. The basic idea of greedy algorithm is to make the locally optimal choice under the current state in each step of selection, hoping to reach the globally optimal result. Based on the dynamic criticality, the SO will choose the most "efficient" municipality to recover next. The "efficiency" here is defined as the increment in the number of students accessing education in a given step divided by the total time needed to accomplish the recovery step, which includes the travel time of the SO to reach its destination, the recovery time due to the operational states of the school in that municipality, the recovery time of the bridges on the path if any, as well as the travel time of the RO. After each recovery step (as shown in Fig. 4), the SO decides the next municipality to recover, by calculating the efficiencies of the remaining unrecovered municipalities and road links, opting for the one with the highest efficiency. In terms of the RO, it will prioritize the recovery of bridges that block the SO's way to the next most efficient choice. In the meantime, a "default criticality for the RO" will also be employed to move it to the next task, while SO is busy in one municipality, which means that the RO will follow the default criticality unless receiving a request from the SO, to avoid idle times. This dynamic recovery strategy is designated as "Greedy".

Based on these alternative priorities, four more recovery strategies (1–4) are proposed by combining ranking criteria (Fig. 9), with the baseline recovery being Strategy 0 (MC1+BC1). Their median recovery trajectories under extreme scenario are compared in Fig. 9. In addition, the "resilience" of the system is also considered [107], computed as the area under the curve within a control time of interest, normalized to 1 (this being the area of the rectangle for the same time). This synthetic value aids the comparison of different strategies benefits. A higher resilience value implies a shorter overall interruption and/or a faster recovery process, and vice versa. The resilience values for strategies 0 to 4 are 0.463, 0.612, 0.343, 0.450, and 0.647 respectively, the control time being the total recovery time of Strategy 0.

Overall, Strategies 1 and 4 outperform Strategy 0 with shorter total recovery times and greater rapidity. Comparing curves 0 to 3, it can be noted that ranking the municipality by damage states (MC2), although provides more granularity in the recovery process, is not more efficient than the ranking based on total number of students (MC1), while linking the RO activity to the SO's needs (BC2), has a significant positive effect on rapidity and total recovery time.

Strategy 4 displays the highest efficiency, with the steepest initial gradient and the highest resilience level. The SO resourcefully chooses the municipalities to maximise the number of students with access to education within the shortest time. However, Strategy 4 does not lead to the shortest total recovery time, because RO's might incur conflicting criticalities in between iterations. In contrast, RO will optimise its recovery efficiency in Strategy 1, as the itinerary of SO is known at the outset, leading to parallel coordinated activity. Such result indicates that the greedy strategy can ensure "local optimisation" but can only reach approximately "global optimisation". Nevertheless, the resilience indicator, as conceived, is still in favour of Strategy 4.

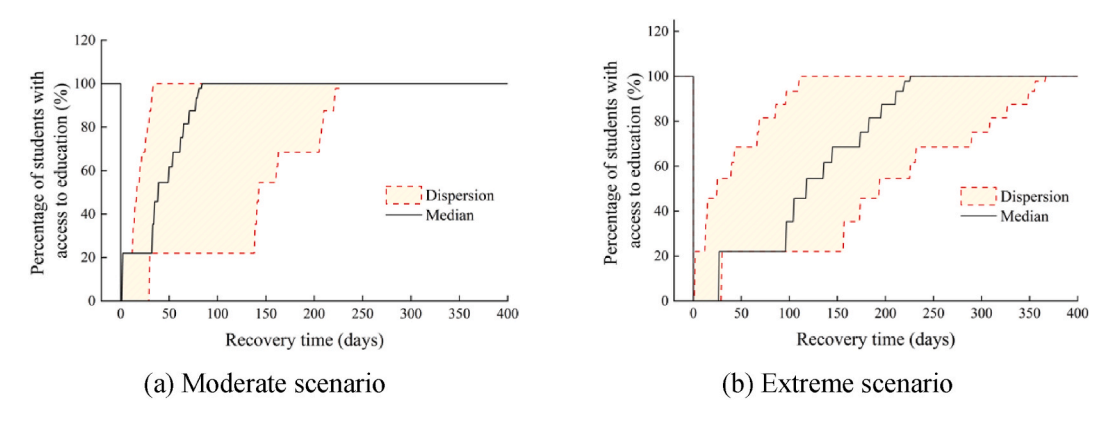


Fig. 8. Recovery trajectories of school operation under seismic scenarios.

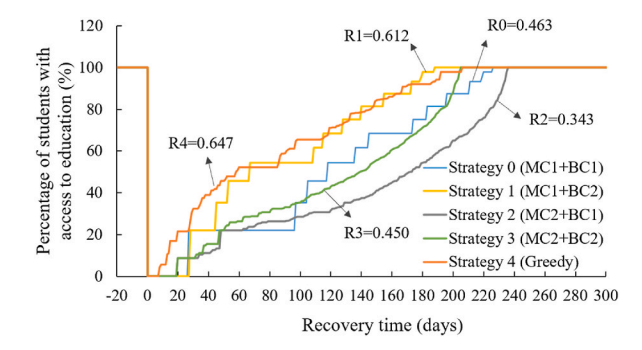


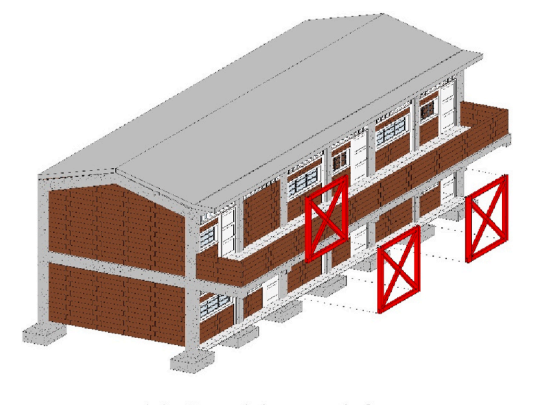
Fig. 9. Recovery trajectories of school operation for different recovery strategies under extreme seismic scenario.

4.3. Retrofitting strategies for school buildings and bridges

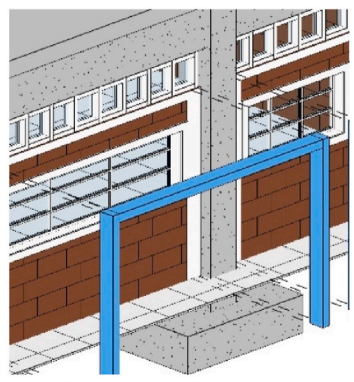
One of the main reasons to investigate system resilience is to provide support to the decision-making for possible investments in school infrastructure strengthening. The objective is to determine whether seismic retrofitting strategies can be useful to mitigate the education service interruption determined in Section 4.2. Some of the typologies of school buildings are more seismically vulnerable than others (Section 4.1), therefore tailored structural interventions can be an efficient risk reduction strategy for the school physical infrastructure, as shown by Fernández et al. [74]. For example, for the typology RC3/MR/LD, short column, low stiffness, weak story, and strong beam-weak column failure mechanisms can be identified. An effective retrofitting approach can be isolating the infill walls and installing steel-braced frames, as shown in Fig. 10. The cost of such intervention is estimated at 30 % of the replacement value. Table 13 presents typology specific structural deficiencies, retrofitting strategy, retrofitting estimated cost and updated fragility functions (for details see Fernández et al., [40]; Fernández et al., [74]). Likewise, Table 14 presents a summary of retrofitting strategies for the bridge typologies and their associated costs (for details see Universidad de Los Andes et al., [79]).

Three retrofitting strategies can be adopted at system level: retrofitting the school buildings, retrofitting the bridges, and retrofitting both. Once the retrofitting strategies are implemented, a new set of MC simulations, sampled on the basis of the BN analysis results informed by the modified fragility functions, is computed, and the AB analysis is performed again, using the Greedy recovery approach defined in Section 4.2, which provided the best system resilience value. The results (median values) are shown in Fig. 11 for both seismic hazard scenarios, while the resilience values are compared in Table 15, using as control time the total recovery time of the original trajectory. While all three retrofitting strategies reduce total recovery times and increase system resilience values, retrofitting both schools and bridges shows best performance. Coincidence can be found in the early stage of the recovery in the curve pairs of *Original* and *Retrofitting bridges* with *Greedy* recovery strategy and the curve pairs of *Retrofitting schools* and *Retrofitting both* in *Extreme scenario* (Fig. 11b). This is because with the *Greedy* recovery approach, SO will choose the most efficient municipality to recover in every step, which allows the most students back to school given the time needed. In the *Extreme scenario*, more bridges fall into higher damage states, in which case the recovery time of a bridge may be much longer than RO's transportation time. Hence, in the early stage of the recovery when the bridges are being recovered, SO will choose paths to municipalities, which may be longer but are not affected by the bridge recovery, to avoid delays. Therefore, for two curve pairs, where the only difference is the retrofitting bridges option, the curves coincide in the early stage of recovery as the sequence of municipalities recovered may be the same.

Nevertheless, it can be noted how retrofitting the bridges is critical to the recovery rapidity of the education in the latter part of the trajectory. This is an expected outcome, considering the fact that without functional bridges the recovery of schools would not be



(a) Steel braced frames



(b) Infills isolation

Fig. 10. Illustrative schemes for RC3/MR/LD retrofitting [74].

Table 13
Seismic retrofitting measures for school buildings. Adapted from Fernández et al. [74].

Typology	Structural deficiency	Retrofitting measure	Estimated cost relative to the replacement value	Updated fragility function
1erBID/RC3/LR/LD	Short column Weak story	- Infills isolation	5 %	1.0 0.8 0.8 0.1 0.2 0.0 0.0 0.0 0.0 0.0 0.0 0.0 0.0 0.0
SEE/RC3/MR/LD	Short column Low stiffness Weak story Strong beam weak column	- Infills isolation - Steel braced frames	30 %	1.0 0.8 0.8 0.8 0.6 0.0 0.0 0.0 0.0 0.0 0.0 0.0 0.0 0.0
PNEE/RC1/MR/HD PNEE/	• No deficiencies	- No intervention	-	
RC1/LR/HD JOHNSON/RM/LR/LD	Low shear capacity Weak connections Out-of-plane failure Low material quality	- Splints and bandage	16 %	0.8 0.8 0.4 0.2 0.2 0.0 0.0 0.5 1.0 1.5 2.0 2.5 PGA [g]
PIDE/RM/LR/LD	 Lack of rigid diaphragm Low shear capacity Weak connections Out-of-plane failure Low material quality 	- Splints and bandage - Tie column	25 %	0.8 0.8 0.8 0.6 0.2 0.0 0.0 0.5 1.0 1.5 2.0 2.5 PGA [g]
PIDE/RM/LR/PD Timber/TF/ LR/LD	High seismic vulnerability	- Replacement	100 %	0.8 Slight Moderate Extensive Collapse 0.0 0.0 0.5 1.0 1.5 2.0 2.5 Sa(T) [g]

possible, as the operators will not be able to access them. Furthermore, bridges and in general the transportation network plays a vital role in the aftermath of a disaster as without it students and the broader academic community and services would not be able to reach the school facilities.

In order to quantitatively assess the impact of each retrofitting strategy, metrics of cost efficiency are provided in Table 16, updated for 2024. The total cost is provided, then divided by the number of days of reduced disruption to identify the cost per reduced day. It can be seen that the retrofitting measures chosen are effective for both levels of seismicity, indeed delivering greater effectiveness for the extreme scenario. However, to have a more synthetic and easy-to-communicate metric, the cost per reduced day is also normalized by the number of students benefitting from it. With this efficiency metric, the most effective strategy, i.e., retrofitting schools and bridges, leads to efficiency costs of \$US 9.80 and \$US 6.71 per student per day of reduced disruption, for the modest and extreme scenario respectively. These are not the most economic solutions, but the ones that maximise the reduction of disruption. Such metric allows to communicate the risk and the benefit of implementing a mitigation measure, with a cost figure that can be easily compared to other educational costs per day per student, such as bus transport, or student's meals. Such metrics can be understood by a nontechnical decision-maker but also clearly communicated to other stakeholders in the community.

Table 14 Seismic retrofitting strategy for bridges.

Typology	Retrofitting measure	Estimated relative cost to the replacement value	Updated fragility functions
Multispan simply supported concrete girder (MSSS Concrete)	Retrofitting of vertical elements Improvement in connections Adding shear keys Neoprene bearing replacement	6.9 %	1.0 0.8 0.8 0.0 0.0 0.0 0.0 0.0 0.0 0.0 0
Multispan simply supported slab with supporting walls (MSSS Slab)		3.1 %	0.8 0.8 0.8 0.6 0.0 0.0 0.0 0.0 0.0 0.0 0.0 0.0 0.0
Multispan continuous concrete girder (MSC Concrete)		3.1 %	0.8 0.8 0.8 0.0 0.0 0.0 0.0 0.0 0.0 0.0
Multispan continuous steel girder (MSC Steel)		5.1 %	0.8 0.8 0.0 0.0 0.0 0.0 0.0 0.0
Multispan simply supported slab with supporting frames (MSSS2 Concrete)		6.9 %	98 0.6
Single span concrete girder (SS Concrete)		4.5 %	1.0 — Maga: —
Cable-stayed bridge (CS)		6.9 %	10 10 10 10 10 10 10 10 10 10 10 10 10 1

5. Interruption of education in flood scenarios and resilience improvement

Regarding the flood case, the affected municipality and road segments susceptible to flooding are identified using the real pathway and schools' locations shown in Fig. 5. Fig. 12 shows the areas susceptible to floods (blue shade) and highlights in red the portion of the topological road network and the two municipalities (M9 and M10) affected. Five road segments (R1 to R5), linking the flood-prone

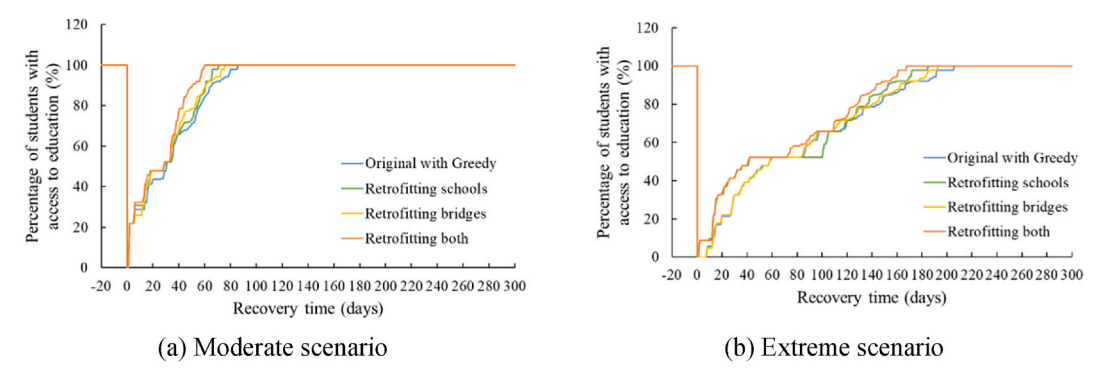


Fig. 11. Recovery trajectories of school operation with different retrofitting strategies under seismic scenarios.

Table 15
Resilience values with different retrofitting strategies under seismic scenarios.

Scenario	Original with Greedy	Retrofitting schools	Retrofitting bridges	Retrofitting both
Moderate	0.625	0.660	0.661	0.705
Extreme	0.647	0.680	0.656	0.706

Table 16Cost efficiency metrics under seismic scenarios.

Scenario	Retrofitting Strategy	Median recovery time (days)	Cost (\$US)	Reduced recovery time days (%)	Cost per reduced day (\$US)	Cost per reduced day per student (\$US)
Moderate	Original with	86	-	-	_	-
	Greedy					
	Retrofitting	71	10,784,846	15 (17.4 %)	718,990	12.83
	Schools					
	Retrofitting	76	3,492,216	10 (11.6 %)	349,222	6.23
	Bridges					
	Retrofitting	60	14,277,062	26 (30.2 %)	549,118	9.80
	Both					
Extreme	Original with	206	_	-	-	_
	Greedy					
	Retrofitting	185	10,784,846	21 (10.2 %)	513,564	9.17
	Schools					
	Retrofitting	193	3,492,216	13 (6.3 %)	268,632	4.80
	Bridges					
	Retrofitting	168	14,277,062	38 (18.4 %)	375,712	6.71
	Both					

municipalities to the province-level road network, are the vulnerable components.

An initial inundation duration of seven days [108], which corresponds to a 50-year return period event [91,95], is considered as the flood scenario. Only after the flood recedes can inundated municipalities and road segments be attended to. The recovery assumed periods for the school infrastructure are shown in Table 8. A 14-day recovery time is set for all the inundated road segments. A set of vulnerability functions developed in the CAPRA framework [109] is used for RC and RM buildings, respectively (see Fig. 13a). These functions provide the mean damage ratio (MDR) for the school buildings as inputs to the BN analysis, and correlated to different functional states as follows: MDR< 10 % – intact, MDR between 10 % and 60 % - partial operation and MDR>60 % - shutdown. All schools in a municipality are assumed to be affected by the same flood depth. The two operators effect the recovery following the criticalities of municipalities and roads, ranked by student numbers (MC1) and road betweenness centrality (RC1) as per the baseline conditions introduced in Section 4.

The extent of interruption of education services under the flood scenario is shown in Fig. 14a. Similar to the earthquake scenarios, a dispersion can also be found showing possible recovery trajectories. The dispersion results from the vulnerability functions used in the BN, which involve both the mean and variance of damage ratios shown in Fig. 13. The median value curve shows a delay between day 3 and day 56 due to the inundation receding time, and the recovery time of road segment R4, as well as the recovery of M10 and M9. Beyond this, the rapidity of the process is high as most municipalities suffer no damage from the flood, needing only a two-day inspection. The minimum, median, and maximum recovery times are 58 days, 75 days, and 100 days respectively, showing the localised impact caused by floods rather than earthquakes.

Alternative criticality rankings are considered for the flood recovery, i.e., ranking of municipalities by damage states (MC2) and

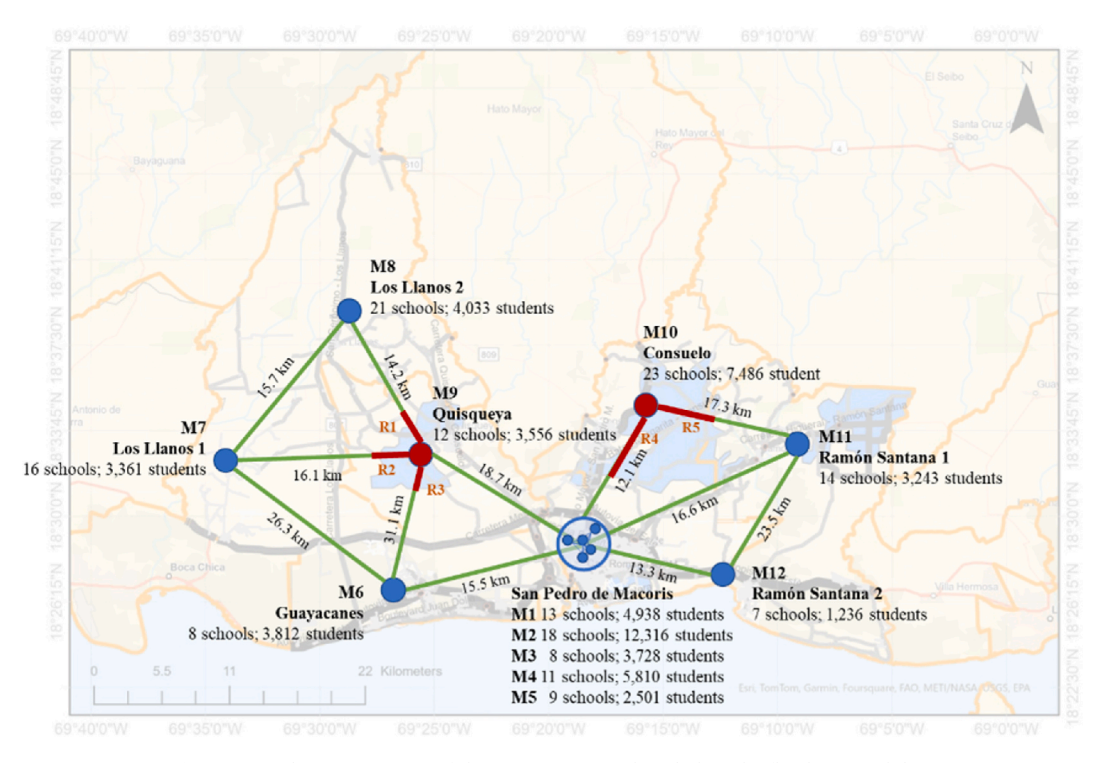


Fig. 12. Graph representation of the province network including the flood susceptibility.

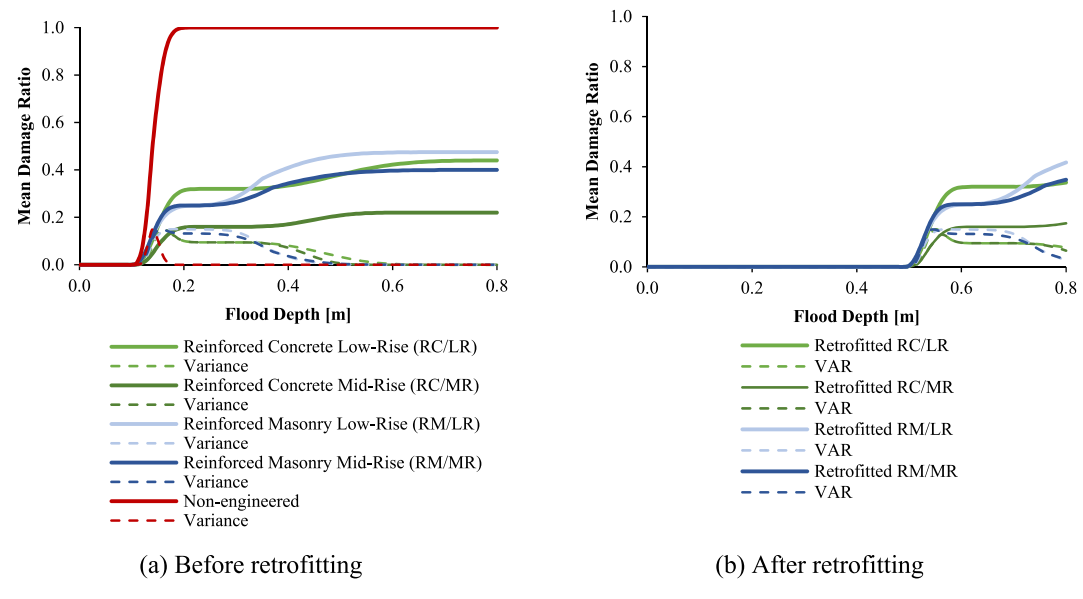


Fig. 13. School buildings flood vulnerability functions. Adapted from CAPRA.

ranking of roads following the criticality of municipalities (RC2). The dynamic criticality based on the greedy algorithm is adopted here as well (Greedy). The same approach used in section 4.2 is used to consider 4 alternative recovery strategies. Fig. 14b shows the corresponding median trajectories. Strategy couples 0–1 and 2–3 curves, perfectly coincide because the ranking of road segments remains the same notwithstanding the different criticality criterion. Therefore, only three curves are visible in Fig. 14b. Ranking municipalities by damage states (Strategies 2 and 3) performs worse initially but concludes with a slightly reduced overall time. The greedy algorithm shows the highest initial efficiency in recovering education services up to 85 % of students, although ending up with a longer total recovery time. Nonetheless, with a control time of 75 days, the resilience value of Strategy 4 is 0.617, substantially higher than the values for Strategy 0 to 3 which are 0.328, 0.328, 0.179, 0.181, respectively.

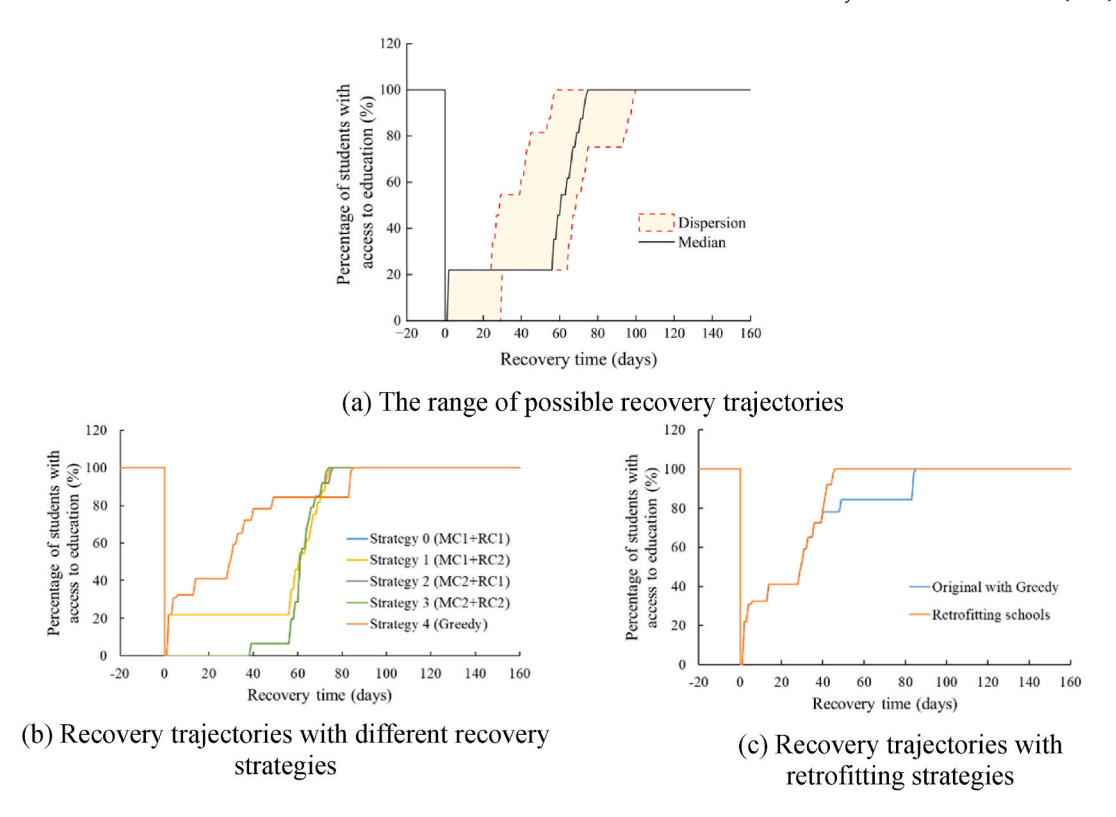


Fig. 14. Recovery trajectories of school operation under flood scenario.

Finally, a dry flood-proofed mitigation strategy is proposed for each school building located in the susceptible area. This solution includes external finishing of walls to make them impervious to floodwater, shields for openings with low thresholds and installations of backflow valves in relevant plumbing [110–112]. These measures are designed for a floodwater depth of 500 mm with an approximate cost of \$US 390/m² of the building footprint, indexed to 2024. A simplified approach to computing the benefit of the measures is to shift the vulnerability functions damage levels by 500 mm of flood depth, as indicated in Fig. 13b. Other mitigation interventions, such as the implementation of flood defences at district or territorial level would also be effective for flood mitigation, but are not considered in this study as the objective is to identify the possible measures taken by a school infrastructure administrator. The roads are also not intervened on, in this scenario. Using Strategy 4, the results for the retrofitted scenario are compared to the original situation in Fig. 14c, highlighting that the retrofitting is effective in eliminating the delay at the end of the recovery campaign. This results in a reduction of the interruption of education service by 45.9 % under the flood scenario, with a cost of \$US 26.04 per reduced day per student affected (see Table 17). On the other hand, the resilience value increases to 0.690 comparable to the values for the seismic scenarios.

6. Further discussion on the method's applicability

Educational interruption has devastating impacts on students and development in countries, as recently highlighted by the vast literature referring to the COVID-19 related school shut down period [113–115]. Governments are increasingly aware of the immediate impact and implications for future development of education disruption, and emergency policies are being developed in the aftermath of major natural disastrous events [17,116,117]. Nonetheless, as shown in this study, while different recovery strategies can reduce the overall disruption period, pre-event investments to improve educational and transport infrastructures are essential to successfully minimise such disruption. Quantifiable information such as the mitigation of a disruption obtained by a given level of

Table 17
Cost efficiency metrics under flood scenarios.

Retrofitting Strategy	Median recovery time (days)	Cost (USD)	Reduced recovery time (days) and percentage	Cost per reduced day (USD)	Cost per reduced day per student (USD)
Original with Greedy	85	-	-	-	-
Retrofitting Schools	46	\$ 11,215,945	39 (45.9 %)	287,588	26.04

investment represents a key metric that can be used to prioritize developmental and risk reduction policies [118,119]. Such metrics can inform national infrastructure governmental planning in the short to medium-term, by identifying the critical assets, municipalities, or provinces in the country that should be prioritized for investment to reduce future risk. This modelling also provides valuable information to international organizations such as UNESCO to provide evidence to the international community of disaster risk levels in different countries and inform international and national governance [120,121]. Finally, international development financing institutions can better tailor lending programmes by using similar methodology to identify investment gaps and prioritize interventions [122]. The application in the present study shows the versatility of using simple metrics to evaluate alternative strategies to optimise resource allocation.

Synthetic and relatable metrics are key elements in risk communication. In the present study the cost of reducing one day of interruption per student is used, and its magnitude, amounting to a few dollars, is easily understood by a non-technical audience and relatable to other typical costs per day per student associated with education such as the cost of school meals or school bus fare. It is therefore much more meaningful than the total number of reduced days or the more conventional expected economic losses, which lack interpretability and need more context, such as the total time of interruption in the existing scenario or the total exposed value of the portfolio.

Nonetheless results should be carefully interpreted. For instance, from the values presented in Sections 4 and 5 it could be concluded that investing in seismic retrofitting is more cost-effective than in flood mitigation measures. However, when considering the frequency of the hazard considered (return period of 475 years for earthquakes and 50 years for floods), it can be seen that investing in reducing flood is about 3.6 times more efficient when the cumulative interruption time is considered. This doesn't mean that school buildings shouldn't be retrofitted for earthquakes, since additional factors such as human lives and asset loss should also be considered but aids the decision maker to weigh different possibilities, within different timeline horizons. Additional approaches such as retrofitting buildings for earthquakes and floods simultaneously or using multi-criteria decision making to choose the most appropriate retrofitting in a multi hazard environment can also be considered as an alternative [123]. Additional analysis such as probabilistic risk assessments also give valuable information to support decision making, as metrics like the Average Annual Losses (AAL) can be used to determine the investment gaps and priorities [124].

The inclusion in the analysis of the supporting infrastructure, such as bridges and roads, provides a systemic lens and allows to consider the value of alternative investment strategies at the regional level. From the results it can be concluded that the road network plays a fundamental role in ensuring or impairing education service delivery. While remote education can be an alternative in emergencies, ensuring mobility to enable in-person education is critical for student development but also for other aspects of societal wellbeing, as demonstrated by Ref. [125]. Moreover, even though this case study only includes the transportation network, the method can be extended to include additional supporting infrastructure networks, such as electricity, water, sewerage, and communications, which directly impact schools' functionality.

The value of the methodology is in its flexible and dynamic approach allowing complex system interaction and multicriteria decision-making under uncertainty to be represented and analysed in a way that is easy to understand by decision-makers and end users, retaining a sufficient degree of fidelity in terms of the structural response to hazards. The figures obtained are a function of the available information. Such figures can be refined if better statistical information is available on population distribution and socioeconomic profile, exposure of the assets and their typological characterisation. While the limitation of subjectivity in the conditional probability definitions in the Bayesian network analysis is acknowledged, its positive aspect is that it allows to trace these uncertainties at each step and retains them in the final outcomes. The analysis can be further improved by considering he correlations between different factors, especially those factors influencing the social vulnerability. A major area of possible improvement relates to the Agent-Based Model, with better data on time, resources and processes needed for the recovery, as currently there is very little consolidated data to accurately represent the complex interactions and decision-making processes that underline recovery timelines for such events.

7. Conclusions

A method to model the recovery of the school infrastructure considering the interaction with the transportation network is developed. This allows to quantify the interruption of the education services following a natural hazardous event. The model includes a Bayesian network (BN), Monte-Carlo simulations (MC), and an Agent-Based model (AB). As a case study, the model is implemented in the province of San Pedro de Macoris in the Dominican Republic, investigating two earthquake scenarios with a uniform PGA of 0.25g (moderate) and 0.6g (extreme), and one flood scenario with a flood water depth of 0.25m. Different recovery and retrofitting strategies are tested, demonstrating the capability of the proposed model to conduct what-if analysis. From this exercise emerges that when the recovery agents in charge of different infrastructures, such as bridges and schools, collaborate, a most efficient recovery process can be obtained. To quantify their effectiveness, a system resilience value and the cost of reducing one day of interruption per student are introduced. This proposed metric has the advantage to be easily understandable by non-technical decision-makers, making it ideal to be used to support retrofitting programs. Besides this objective, these types of metrics can be used to effectively communicate risk to broader audiences to support preparedness policies.

The proposed methodology and the implementation presented herein are susceptible of improvement. For instance, the current implementation uses constant values of hazard for exposed locations, in the absence of more refined models. It also includes basic assumptions on recovery time given an operational state. The impact of these assumptions on the total time of recovery of the educational services should be further investigated, using archival information and in-country local experience. The method is sufficiently flexible to warrant application to other natural hazards, and different geographical scales, by increasing or reducing the

granularity of the information. A multi-hazard country-level application, for instance, could be helpful to identify regional infrastructure most susceptible to specific hazards, to better tailor local investments and policies.

CRediT authorship contribution statement

Dina D'Ayala: Writing – review & editing, Writing – original draft, Visualization, Validation, Supervision, Project administration, Methodology, Funding acquisition, Conceptualization. Rafael Fernández: Writing – review & editing, Writing – original draft, Validation, Supervision, Resources, Project administration, Methodology, Investigation, Formal analysis, Data curation, Conceptualization. Ahsana Parammal Vatteri: Writing – review & editing, Writing – original draft, Visualization, Software, Methodology, Investigation, Formal analysis, Data curation, Conceptualization. Zaishang Li: Writing – review & editing, Writing – original draft, Visualization, Validation, Software, Methodology, Funding acquisition, Conceptualization. Soichiro Yasukawa: Visualization, Validation, Funding acquisition, Conceptualization.

Data availability statement

The data used in this paper for the case study is not publicly available as the authors do not have the permission to publish it but can be provided individually if requested. Additional inputs used in this implementation can be found in their original references: seismic hazard model [84], flood hazard model [91], fragility functions for schools [40,74,75], fragility functions for bridges [78,80], vulnerability functions for floods [109], seismic retrofitting of school buildings [74], flood retrofitting of school buildings [111], and bridge retrofitting [79].

Declaration of competing interest

The authors declare the following financial interests/personal relationships which may be considered as potential competing interests: Dina D'Ayala reports financial support was provided by United Nations Educational Scientific and Cultural Organization. If there are other authors, they declare that they have no known competing financial interests or personal relationships that could have appeared to influence the work reported in this paper.

Acknowledgments

This study was developed within the framework of the BERLAC project (Capacity Building for Disaster Risk Reduction in the Built Environment in Latin America and the Caribbean), funded by the UNESCO Disaster Risk Reduction Unit with initial funding from the Government of Japan. Authors also would like to express their gratitude to ONESVIE and the Ministry of Education in the Dominican Republican. Both institutions had a critical role in gathering information and understanding the local context. Authors gladly acknowledge the support of the UNESCO Chair in Disaster Risk Reduction and Resilience Engineering, which funds some of their time.

Data availability

Data will be made available on request.

References

- [1] Human Rights Council, Impact of Climate Change on the Equal Enjoyment of the Right to Education by Every Girl (A/HRC/57/37), United Nations General Assembly, 2024.
- [2] H. Baytiyeh, Online learning during post-earthquake school closures, Disaster Prev. Manag. 27 (2) (3 2018) 215-227.
- [3] E. Segarra, J. Caraballo-Cueto, Y. Cordero, H. Cordero, The effect of consecutive disasters on educational outcomes, Int. J. Disaster Risk Reduct. 83 (2022).
- [4] R. López, J. Martínez, Damages observed in Puerto Plata, Dominican Republic, due to the September 22, 2003 earthquake, Revista internaciona de Desastres Naturales, Accidentes e Infraestructura Civil (2003) 189–204.
- [5] E. Munsaka, S. Mutasa, Flooding and its impact on education, in: Natural Hazards Impacts, Adjustments and Resilience, 2020.
- [6] J. Lassa, M. Petal, A. Surjan, Understanding the impacts of floods on learning quality school facilities and educational, Disasters 47 (2) (2022) 412-436.
- [7] A. Anderson, G. Martone, J.P. Robinson, E. Rognerud, J. Sullivan-Owomoyela, Standards Put to the Test: Implementing the INEE Minimum Standards for Education in Emergencies, Chronic Crisis and Early Reconstruction, vol. 57, Humanitarian Practice Network at ODI, 2006, pp. 1–28.
- [8] K. Thamtanajit, The impacts of natural disaster on student achievement: evidence from severe floods in Thailand, J. Develop. Area. 54 (4) (2020).
- [9] L. Gibbs, J. Nursey, J. Cook, G. Ireton, N. Alkemade, M. Roberts, H.C. Gallagher, R. Bryant, Delayed disaster impacts on academic performance of primary school children, Child Dev. 90 (4) (2019) 1402–1412.
- [10] K.A. Shidiqi, A. Di Paolo, A. Choi, Earthquake Exposure and Schooling: Impacts and Mechanisms, Elsevier Ltd, 2023.
- [11] H. Baytiyeh, Why school resilience should be critical for the post-earthquake recovery, Educ. Urban Soc. 51 (5) (2019) 693-711.
- [12] D. D'Ayala, C. Galasso, A. Nassirpour, R.R.K. Adhikari, L. Yamin, R. Fernandez, D. Lo, L. Garciano, A. Oreta, Resilient communities through safer schools [Online]. Available: https://doi.org/10.1016/j.ijdrr.2019.101446, 2020.
- [13] Undrr, Resilience, 2023 [Online]. Available: https://www.undrr.org/terminology/resilience.
- [14] S. Mirzaei, L. Mohammadinia, K. Nasiriani, A.A.D. Tafti, Z. Rahaei, H. Falahzade, H.R. Amiri, School resilience components in disasters and emergencies: a systematic review, Trauma Mon. 24 (5) (2019).
- [15] S. Mirzaei, H. Falahzade, L. Mohammadinia, K. Nasiriani, A. Dehghani Tafti, Z. Rahaei, H. Amiri, Assessment of school resilience in disasters: a cross-sectional study, J. Educ. Health Promot. 9 (1) (2020) 1.
- [16] C. Fontana, E. Cianci, M. Moscatelli, Assessing seismic resilience of school educational sector. An attempt to establish the initial conditions in Calabria Region, southern Italy, Int. J. Disaster Risk Reduct. 51 (12) (2020).

- [17] E.M. Hassan, H.N. Mahmoud, B.R. Ellingwood, Resilience of school systems following severe earthquakes, Earths Future 8 (10) (2020), 10.
- [18] C. González, M. Niño, M.A. Jaimes, Event-based assessment of seismic resilience in Mexican school buildings, Bull. Earthq. Eng. 18 (14) (2020) 6313–6336, 11.
- [19] D. Samadian, M. Ghafory-Ashtiany, H. Naderpour, M. Eghbali, Seismic resilience evaluation based on vulnerability curves for existing and retrofitted typical RC school buildings, Soil Dynam. Earthq. Eng. 127 (12) (2019).
- [20] F.L. Ribeiro, P.X. Candeias, A.A. Correia, A.R. Carvalho, A.C. Costa, Risk and resilience assessment of Lisbon's school buildings based on seismic scenarios, Applied Sciences (Switzerland) 12 (17) (2022), 9.
- [21] W.W. Carofilis Gallo, N. Clemett, G. Gabbianelli, G. O'reilly, R. Monteiro, Seismic resilience assessment in optimally integrated retrofitting of existing school buildings in Italy, Buildings 12 (6) (2022), 6.
- [22] L. Sun, D. D'Ayala, R. Fayjaloun, P. Gehl, Agent-Based Model on resilience-oriented Rapid Responses of Road Networks Under Seismic Hazard, Reliab Eng Syst Saf. 2021
- [23] D. McKoy, J.M. Vincent, C. Makarewicz, Integrating infrastructure planning: the role of schools, ACCESS Magazine 1 (33) (2008).
- [24] J.B. Wagner, "Impact of School Location on Transportation Infrastructure and Finance," Atlanta, 2009.
- [25] C. Sundstrom, N. Pullen-Seufert, M. Cornog, M. Cynecki, K. Chang, Prioritizing Schools for Safe Routes to School Infrastructure Projects, ITE Journal, 2010.
- [26] D. D'Ayala, R. Fernández, A. Parammal Vatteri, S. Yasukawa, A. Bendito, Minimize Education Disruption Following Natural Hazards, UNESCO, 2023.
- [27] M. Bensi, A. Der Kiureghian, D. Straub, A Bayesian Network Methodology for Infrastructure Seismic Risk Assessment and Decision Support, Report No. 2011/02, Pacific Earthquake Engineering Research Center, University of California, Berkeley, 2011.
- [28] P.L. Bonate, A brief introduction to Monte Carlo simulation, Clin. Pharmacokinet. 40 (1) (2001) 15-22.
- [29] C.M. Macal, M.J. North, Tutorial on agent-based modeling and simulation, in: Proceedings of the Winter Simulation Conference, 2005. Orlando, FL, USA.
- [30] A.J. Pope, R. Gimblett, Linking Bayesian and agent-based models to simulate complex social-ecological systems in semi-arid regions, Front. Environ. Sci. 3 (2015), https://doi.org/10.3389/fenvs.2015.00055.
- [31] S.A. Abdulkareem, Y.T. Mustafa, E.W. Augustijn, Bayesian networks for spatial learning: a workflow on using limited survey data for intelligent learning in spatial agent-based models, GeoInformatica 23 (2019) 243–268.
- [32] V. Kocabas, S. Dragicevic, Bayesian networks and agent-based modeling approach for urban land-use and population density change: a BNAS model, J. Geogr. Syst. 15 (2013) 403–426.
- [33] T. Haer, W.J. Botzen, H. de Moel, J.C. Aerts, Integrating household risk mitigation behavior in flood risk analysis: an agent-based model approach, Risk Analysis 37 (2017) 1977–1992.
- [34] B. Marcot, T. Penman, Advances in Bayesian network modelling: integration of modelling technologies, Environ. Model. Software 111 (2019) 386-393.
- [35] P. Gehl, D. D'Ayala, System loss assessment of bridge networks accounting for multi-hazard interactions, Structure and Infrastructure Engineering 14 (10) (2018) 1355–1371.
- [36] J.E. Byun, D. D'Ayala, Urban seismic resilience mapping: a transportation network in Istanbul, Turkey, Sci. Rep. 12 (1) (2022), 12.
- [37] A. Parammal Vatteri, D. D'Ayala, P. Gehl, Bayesian networks for the assessment of disruption to school systems under combined hazards, Int. J. Disaster Risk Reduct. 74 (2022), https://doi.org/10.1016/j.ijdrr.2022.102924.
- [38] R.J. Dawson, R. Peppe, M. Wang, An agent-based model for risk-based flood incident management, Nat. Hazards 59 (2011) 167–189.
- [39] S. Ghaffarian, D. Roy, T. Filatova, N. Kerle, Agent-based modelling of post-disaster recovery with remote sensing data, Int. J. Disaster Risk Reduct. 60 (2021) 102285.
- [40] R. Fernández, L.E. Yamin, D. D'Ayala, R.K. Adhikari, J.C. Reyes, J. Echeverry, G. Fuentes, A simplified component-based methodology for the seismic vulnerability assessment of school buildings using nonlinear static procedures: application to RC school buildings, Bull. Earthq. Eng. 20 (2022) 6555–6585, https://doi.org/10.1007/s10518-022-01445-5.
- [41] A. Fothergill, L.A. Peek, Poverty and disasters in the United States: a review of recent sociological findings, Nat. Hazards 32 (2004) 89-110.
- [42] C. Mudavanhu, The impact of flood disasters on child education in Muzarabani District, Zimbabwe, Jàmbá: Journal of Disaster Risk 6 (1) (2014) 1-8.
- [43] M.C. de Ruiter, A. Couasnon, M.J.C. van den Homberg, J.E. Daniell, J.C. Gill, P.J. Ward, Why we can no longer ignore consecutive disasters, Earths Future 8 (2020).
- [44] B.E. Flanagan, E.W. Gregory, E.J. Hallisey, J.L. Heitgerd, B. Lewis, A social vulnerability index for disaster management, J. Homel. Secur. Emerg. Manag. 8 (1) (2011).
- [45] F. Fatemi, A. Ardalan, B. Aguirre, N. Mansouri, I. Mohammadfam, Social vulnerability indicators in disasters: findings from a systematic review, Int. J. Disaster Risk Reduct. 22 (2017) 219–227.
- [46] W. Utami, Study of social vulnerability as an effort on disaster risk reduction (study on suburban communities in Yogyakarta, Indonesia), IOP Conf. Ser. Earth Environ. Sci. 243 (2019) 012014.
- [47] Y. Ge, W. Dou, Z. Gu, X. Qian, J. Wang, W. Xu, P. Shi, X. Ming, X. Zhou, C. Yuan, Assessment of social vulnerability to natural hazards in the Yangtze River Delta, China, Stoch. Environ. Res. Risk Assess. (2013) 1899–1908.
- [48] S.L. Cutter, B.J. Boruff, W.L. Shirley, Social vulnerability to environmental hazards, Soc. Sci. Q. 84 (2) (2003) 242–261.
- [49] Y. Wei, Y. Fan, C. Lu, H. Tsai, The assessment of vulnerability to natural disasters in China by using the DEA method, Environ. Impact Assess. Rev. 24 (4) (2004) 427–439.
- [50] D.C. Roy, T. Blaschke, A grid-based approach for spatial vulnerability assessment to floods: a case study on the coastal area of Bangladesh, in: GI4DM Conference, 2011. Antalya.
- [51] Y.-J. Lee, Social vulnerability indicators as a sustainable planning tool, Environ. Impact Assess. Rev. (2014) 31-42.
- [52] J. Crowley, Social vulnerability factors and reported post-disaster needs in the aftermath of Hurricane florence, International Journal of Disaster Risk Science 12 (1) (2 2021) 13–23.
- [53] V. van der Land, D. Hummel, Vulnerability and the role of education in environmentally induced migration in Mali and Senegal, Ecol. Soc. 18 (4) (2013).
- [54] W. Chen, S.L. Cutter, C.T. Emrich, P. Shi, Measuring social vulnerability to natural hazards in the Yangtze River Delta region, China, International Journal of Disaster Risk Science 4 (4) (2013) 169–181.
- [55] R. Muttarak, W. Lutz, Is education a key to reducing vulnerability to natural disasters and hence unavoidable climate change? Ecol. Soc. 19 (1) (2014).
- [56] D.M. Drzewiecki, H.M. Wavering, G.R. Milbrath, V.L. Freeman, J.Y. Lin, The association between educational attainment and resilience to natural hazard-induced disasters in the West Indies: st. Kitts & Nevis, Int. J. Disaster Risk Reduct. 47 (8) (2020).
- [57] E. Frankenberg, B. Sikoki, C. Sumantri, W. Suriastini, D. Thomas, Education, vulnerability, and resilience after a natural disaster, Ecol. Soc. 18 (2) (2013).
- [58] S. Rao, F.C. Doherty, S. Teixeira, D.T. Takeuchi, S. Pandey, Social and structural vulnerabilities: associations with disaster readiness, Glob. Environ. Change 78 (1) (2023).
- [59] W.G. Peacock, N. Dash, Y. Zhang, Sheltering and housing recovery following disaster, Handbook of Disaster Research (2007) 258-274.
- [60] P. Weber, G. Medina-Oliva, C. Simon, B. Iung, Overview on Bayesian networks applications for dependability, risk analysis and maintenance areas, Eng. Appl. Artif. Intell. 25 (4) (2012) 671–682.
- [61] S. Mahadevan, R. Zhang, N. Smith, Bayesian networks for system reliability reassessment, Struct. Saf. 23 (3) (2001) 231-251.
- [62] E. Munsaka, S. Mutasa. Flooding and its impact on education, Natural Hazards Impacts, Adjustments and Resilience, 2020. https://doi.org/10.5772/intechopen.94368.
- [63] A. Parammal Vatteri, Performance Assessment of Masonry School Buildings to Seismic and Flood Hazards Using Bayesian Networks, University College London, 2022.
- [64] A. Dunant, M. Bebbington, T. Davies, P. Horton, Multihazards scenario generator: a network-based simulation of natural disasters, Risk Anal. 41 (11) (2021) 2154–2176, 11.
- [65] J. Liu, S. Li, J. Wu, X. Liu, J. Zhang, Research of influence of sample size on normal information diffusion based on the Monte Carlo method: risk assessment for natural disasters, Environ. Earth Sci. 77 (13) (2018), 7.

- [66] J. Baker, B. Bradley, P. Stafford, Seismic Hazard and Risk Analysis, Cambridge University Press, 2022.
- [67] C. Li, G. Wang, J. He, Y. Wang, A novel approach to probabilistic seismic landslide hazard mapping using Monte Carlo simulations, Eng. Geol. 301 (5) (2022).
- [68] X. Xie, B. Xie, J. Cheng, Q. Chu, T. Dooling, A simple Monte Carlo method for estimating the chance of a cyclone impact, Nat. Hazards 107 (3) (7 2021) 2573–2582.
- [69] B. Calvo, F. Savi, A real-world application of Monte Carlo procedure for debris flow risk assessment, Comput. Geosci, 35 (5) (5 2009) 967-977.
- [70] D. D'Ayala, A. Meslem, D. Vamvatsikos, K. Porter, T. Rossetto, H. Crowley, V. Silva, Guidelines for Analytical Vulnerability Assessment Low/Mid-Rise, vol. 12, GEM Technical Report, 2015, p. 162.
- [71] H.K. Mistry, D. Lombardi, A stochastic exposure model for seismic risk assessment and pricing of catastrophe bonds, Nat. Hazards 117 (1) (5 2023) 803–829.
- [72] E.Y. Mentese, G. Cremen, R. Gentile, C. Galasso, E.M. Filippi, J. McCloskey, Future exposure modelling for risk-informed decision making in urban planning, Int. J. Disaster Risk Reduct. 90 (5) (2023).
- [73] Oficina nacional de estadística, Datos y estadísticas demográficos, económicos y sociales en República Dominicana [Online]. Available: https://www.one.gob.do/datos-y-estadísticas/, February 2023.
- [74] R. Fernández, J.F. Correal, D. D'Ayala, A.L. Medaglia, Towards disaster risk mitigation on large-scale school intervention programs, Int. J. Disaster Risk Reduct. 90 (2023), https://doi.org/10.1016/j.ijdrr.2023.103655.
- [75] R. Adhikari, D. D'Ayala, R. Fernández, L. Yamin, A. Nassirpour, A.P. Vatteri, C. Ferreria, F. Ramírez, GLOSI taxonomy: a tool for 'seismic risk assessment' oriented classification of school buildings, Int. J. Disaster Risk Reduct. 87 (2023).
- [76] J.C. Olaya, A. Suardi, B. Lefevre, M. Rodríguez. Transporte Resiliente al Cambio Climático: ¿cómo priorizar la inversión? el caso de República Dominicana, 2022. Banco Interamericano de Desarrollo IDB-TN-02583, https://doi.org/10.18235/0004576.
- [77] OCHA, Humanitarian Data Exchange (HDX) [Online]. Available: https://data.humdata.org/dataset/hotosm.dom.roads, January 2023.
- [78] B.G. Nielson, R. DesRoches, Analytical seismic fragility curves for typical bridges in the central and Southeastern United States, Earthq. Spectra 23 (3) (2007) 615–633.
- [79] Universidad de Los Andes, Universidad Javeriana & INVIAS, "Sistema Inteligente de Gestión de Puentes Para Colombia," Bogotá, 2022.
- [80] W. Wu, L. Li, X. Shao, Seismic assessment of medium-span concrete cable-stayed bridges using the component and System fragility functions, J. Bridge Eng. 21 (6) (2016), 6.
- [81] Ministry of Presidency Dominican Republic, Summary of Infrastructure Investments in the Province of San Pedro de Macoris, Santo Domingo, 2023.
- [82] USGS, Eathquake catalogue [Online]. Available: https://earthquake.usgs.gov/earthquakes/search/, 2019.
- [83] CRED UCLouvain, EM-DAT [Online]. Available: https://www.emdat.be/, 2023.
- [84] K. Johnson, M. Pagani, T. Chartier. Probabilistic seismic hazard model for the Dominican Republic, Global Earthquake Model (GEM), Foundation, 2022. https://www.globalquakemodel.org/product/dominican-republic-hazard.
- [85] D. Bertil, M. Terrier, M. Belvaux, Análisis de las fuentes sísmicas y evaluación de la amenaza sísmica regional del gran Santo Domingo. "Estudio de la Amenaza Sísmica y Vulnerabilidad Física del Gran Santo Domingo" Actividad 1.1, 2015. BRGM/RP-65305-FR.
- [86] O. Benito, B. Cervera, P. Molina, B. Navarro, L. Doblas, D. Martínez, "Évaluation de l'aléa et du risque sismique en Haïti dirigée vers la conception Parasismique,", 2012.
- [87] E.R.N.-A.L. Consorcio, Evaluación del Riesgo Catastrófico en la República Dominicana, 2012.
- [88] MOPC, Reglamento Para el Análisis y Diseño Sísmico de Estructuras, Santo Domingo, 2011.
- [89] A. Frankel, S. Harmsen, C. Mueller, E. Calais, J. Haase, Documentation for Initial Seismic Hazard Maps for Haiti, vols. 2010–1067, U.S. Geological Survey Open-File Report, 2010.
- [90] UNDRR & DESINVENTAR, Desinventar Sendai [Online]. Available: https://www.desinventar.net/DesInventar/profiletab.jsp?countrycode=dom&continue=y, 2023.
- [91] R. Rivera, S. Hernández. Estudio y mapeo de zonas bajo amenazas de inundaciones de la República Dominicana, Ministerio de Medio Ambiente y Recursos Naturales, 2022. https://byearmb.do/handle/123456789/2131.
- [92] N. Gómez, P. Saenz, Análisis de Riesgos de desastres y vulnerabilidades en la República Dominicana, Comisión Europea Ayuda humanitaria, 2009.
- [93] BID, Mapa de amenazas por inundaciones, vol.1152, Sub programa prevención de desastres Préstamo BID, 2000.
- [94] The World Bank, Evaluación de riesgo por sismo y viento huracanado y planes de reducción del riesgo para la infraestructura educativa pública de República Dominicana, 2020.
- [95] DGOT, Amenazas y Riesgos Naturales República Dominican compendio de Mapas. Dirección General de Ordenamiento y Desarrollo Ministerio de Economía, Planificación y Desarrollo, 2012.
- [96] L. Greubel, X. Ackerman, R. Winthrop, Prioritizing education in the face of natural disasters [Online]. Available: https://www.brookings.edu/articles/prioritizing-education-in-the-face-of-natural-disasters/, 31 October 2012.
- [97] P.D.M. Ozer, D.S. Sensoy, D.H.E. Suna, The Impact of Post-disaster Education Management for the Recovery of a Region Following the February 6 2023 Earthquake in Turkiye, TRT World Research Centre, 2023.
- [98] B.S. Lai, A.M. Esnard, C. Wyczalkowski, R. Savage, H. Shah, Trajectories of school recovery after a natural disaster: risk and protective factors, Risk Hazards Crisis Publ. Pol. 10 (1) (2019) 32–51.
- [99] Theirworld, Safe schools: getting children back into education after disaster strikes [Online]. Available: https://theirworld.org/news/safe-schools-getting-children-back-into-education-after-natural-disaster/, 2018.
- [100] A. Tsioulou, J. Faure Walker, D.S. Lo, R. Yore, A Method for Determining the Suitability of Schools as Evacuation Shelters and Aid Distribution Hubs Following Disasters: Case Study from Cagayan De Oro, Philippines, Springer Netherlands, 2021.
- [101] WVLT8, Portion of Foothills Parkway closes for additional inspections after earthquake [Online]. Available: https://www.wvlt.tv/2025/05/14/portion-foothills-parkway-closes-additional-inspections-after-earthquake/, 2025. (Accessed 15 May 2025).
- [102] M. Puleo, How were roads in Alaska repaired so quickly after the earthquake? AccuWeather (2018) [Online]. Available: https://www.accuweather.com/en/weather-news/how-were-roads-in-alaska-repaired-so-quickly-after-the-earthquake/339727#:~:text=This%20combination%20photo%20shows%20a,Photo%2FDan%20Joling%2C%20Mike%20Dinneen%2C%20File. (Accessed 15 May 2025).
- [103] New York State DOT, Governor hochul celebrates reopening of the popolopen Bridge along U.S. route 9W in Orange County following devastating rains, New York State Department of Transportation (4 August 2024) [Online]. Available: https://www.governor.ny.gov/news/governor-hochul-celebrates-reopening-popolopen-bridge-along-us-route-9w-orange-county#:~:text=State%20Department%20of%20Transportation%20Rebuilt,in%20Less%20Than%20Four% 20Weeks. (Accessed 15 May 2025).
- [104] RNZ, Flood-destroyed bridge in Auckland replaced with temporary fix in under a week, Radio New Zealand (8 February 2023) [Online]. Available: https://www.rnz.co.nz/news/national/483856/flood-destroyed-bridge-in-auckland-replaced-with-temporary-fix-in-under-a-week. (Accessed 15 May 2025).
- [105] BBC, Yorkshire Dales: Collapsed bridge Reopens After Flood Repairs, British Broadcast Company, 6 March 2021 [Online]. Available: https://www.bbc.co.uk/news/uk-england-york-north-yorkshire-56306608. (Accessed 15 May 2025).
- [106] P.E. Black, Greedy algorithm [Online]. Available: https://www.nist.gov/dads/HTML/greedyalgo.html, 2 February 2005. (Accessed 21 August 2024).
- [107] Z. Li, N. Li, G.P. Cimellaro, D. Fang, System dynamics modeling-based approach for assessing seismic resilience of hospitals: methodology and a case in China, J. Manag. Eng. 36 (5) (2020) 04020050.
- [108] N. Najibi, N. Devineni, Recent trends in the frequency and duration of global floods, Earth System Dynamics (2018) 757–783.
- $[109] \quad CAPRA, Comprehensive approach for probabilistic risk assessment. \ https://ecapra.org/, 2018, 2023.$
- [110] J.C. Aerts, W.J. Botzen, H. de Moel, M. Bowman, Cost estimates for flood resilience and protection strategies in New York City, Ann. N. Y. Acad. Sci. 1294 (1) (2013) 1–104.
- [111] FEMA, Homeowner's Guide to Retrofitting FEMA P-312, 2014.
- $\textbf{[112]} \ \ \text{J.C. Aerts, A review of cost estimates for flood adaptation, Water (Switzerland) 10 (11) (2018), 11.$

- [113] C. König, A. Frey, The impact of COVID-19-Related school closures on student Achievement—A meta-analysis, Educ. Meas. 41 (1) (2022) 16–22.
- [114] F. Sultana, R. Bari, S. Munir, Impact of school closures due to COVID-19 on education in low- and middle-income countries, J. Glob. Health Rep. 6 (2022).
- [115] D. Mazrekaj, K. De Witte, The impact of school closures on learning and mental health of children: lessons from the COVID-19 pandemic, Perspect. Psychol. Sci. 19 (2023), https://doi.org/10.1177/17456916231181108.
- [116] M. Özer, S. Şensoy, E. Suna, The Impact of Post-disaster Education Management for the Recovery of a Region Following the February 6 2023 Earthquakes in Türkiye, 2023.
- [117] I. Alisjahbana, A. Graur, I. Lo, A. Kiremidjian, Optimizing Strategies for Post-disaster Reconstruction of School Systems, Elsevier Ltd, 2022.
- [118] M.C. Comerio, Estimating downtime in loss modeling, Earthq. Spectra 22 (2) (2006) 349–365.
- [119] S. Prabhu, M. Javanbarg, M. Lehmann, S. Atamturktur, Multi-peril risk assessment for business downtime of industrial facilities, Nat. Hazards 97 (3) (7 2019) 1327–1356.
- [120] UNESCO, Towards resilient non-engineered construction: guide for risk-informed policy-making. UNESCO Disaster Risk Reduction Unit, 2016.
- [121] UNESCO, BERLAC Project: Capacity Building for Disaster Risk Reduction in the Built Environment in Latin America and the Caribbean, 2024.
- [122] The World Bank, Roadmap for safer and resilient schools (RSRS) [Online]. Available: https://gpss.worldbank.org/roadmap-step/school-infrastructure-baseline, 2024.
- [123] A. FathiAzar, S. De Angeli, S. Cattari, Towards integrated multi-risk reduction strategies: a catalog of flood and earthquake risk mitigation measures at the building and neighborhood scales, Int. J. Disaster Risk Reduct. 113 (2024), https://doi.org/10.1016/j.ijdrr.2024.104884.
- [124] ADB, Narrowing the Disaster Risk Protec Tion Gap in Centra l AsiaGap in Central Asia, Asian Development Bank, Metro Manila, Philippines, 2022.
- [125] C. Halloran, R. Jack, J.C. Okun, E. Oster, Pandemic Schooling Mode and Student Test Scores: Evidence from US States, National Bureau of Economic Research, 2021.